



**Environmental
Science**
Processes & Impacts

**Non-Targeted Identification and Semi-Quantitation of
Emerging Per- and Polyfluoroalkyl Substances (PFAS) in US
Rainwater**

Journal:	<i>Environmental Science: Processes & Impacts</i>
Manuscript ID	EM-ART-08-2022-000349.R1
Article Type:	Paper

SCHOLARONE™
Manuscripts

Non-Targeted Identification and Semi-Quantitation of Emerging Per- and Polyfluoroalkyl Substances (PFAS) in US Rainwater

Yubin Kim,^a Kyndal A. Pike,^{a,b,c} Rebekah Gray,^a Jameson W. Sprankle,^{a,d} Jennifer A. Faust,^a
Paul L. Edmiston^{*a}

ABSTRACT

High-resolution mass spectrometry was used to screen for emerging per- and polyfluorinated alkyl substances (PFAS) in precipitation samples collected in summer 2019 at seven sites in the United States. We previously quantified the concentration of ten PFAS in the rainwater samples using the method of isotopic dilution (Pike et al., 2021). Nine of these targeted analytes belonged to the U.S. Environmental Protection Agency Regional Screening Level list, herein referred to as EPA-monitored analytes. In this new work, we identify emerging PFAS compounds by liquid chromatography quadrupole time-of-flight mass spectrometry. Several emerging PFAS were detected across all samples, with the most prevalent compounds being C3-C8 hydrogen-substituted perfluorocarboxylic acids (H-PFCAs) and fluorotelomer carboxylic acids (FTCAs). Concentrations of emerging PFAS were in the 10-1,000 ng L⁻¹ range (approximately 1-2 orders of magnitude greater than EPA-monitored PFAS) at all sites except Wooster, OH, where concentrations were even higher, with a maximum estimated Σ_{PFAS} of

^a Department of Chemistry, College of Wooster, Wooster, OH, USA

^b Department of Mathematical & Computational Sciences, College of Wooster, Wooster, OH, USA

^c Current affiliation: Department of Chemistry, University of Wisconsin-Madison, Madison, WI, USA

^d Department of Earth Sciences, College of Wooster, Wooster, OH, USA

* Corresponding author: pedmiston@wooster.edu

1
2
3
4 16,400 ng L⁻¹. The elevated levels of emerging PFAS in the Wooster samples were
5
6
7 predominantly even and odd chain-length H-PFCAs and FTCAs comprised of complex mixtures
8
9
10 of branched isomers. This unique composition did not match any known manufactured PFAS
11
12
13 formulation reported to date, but it could represent thermally transformed by-products emitted by
14
15
16 a local point source. Overall, the results indicate that PFAS outside of the standard analyte lists
17
18
19 make up a significant and previously unappreciated fraction of contaminants in rainwater
20
21
22 collected within the central U.S.—and potentially world-wide—especially in proximity to
23
24
25
26
27 localized point sources.
28
29
30
31

32 **ENVIRONMENTAL SIGNIFICANCE**

33

34 PFAS, or per- and polyfluorinated alkyl substances, are ubiquitous chemicals that are both toxic
35
36 to humans and long-lived in the environment. Typically only a handful of PFAS are routinely
37
38 monitored in the environment, and only four are regulated in drinking water across the United
39
40 States. Here we used high-resolution mass spectrometry to identify over 20 emerging PFAS in
41
42 rainwater samples from seven U.S. sites. (Note: Emerging PFAS is defined as compounds that
43
44 do not appear as EPA Method 533 and/or 537.1 analytes.) The most prevalent PFAS were highly
45
46 branched polyfluorinated carboxylic acids. Wet deposition of these compounds from the
47
48 atmosphere could represent an important yet ignored source of PFAS contamination. Results
49
50 from our regional sampling network suggest that local point sources exert a significant influence
51
52
53 on the isomeric profiles and deposition fluxes of PFAS in precipitation.
54
55
56
57
58
59
60

INTRODUCTION

PFAS, or per- and polyfluoroalkyl substances, are anthropogenic chemicals with a wide variety of uses, ranging from manufacturing to consumer products to firefighting.¹ PFAS are highly persistent in the environment, and they can enter the atmosphere through direct emissions or through degradation of precursors.^{2,3} Once in the atmosphere, PFAS and their precursors can undergo long-range transport in the gas phase or in the particle phase and return to Earth through wet and dry deposition.⁴⁻⁹ Accordingly, PFAS have been detected at remote locations such as the Arctic,^{5,10-13} the Antarctic,^{14,15} and open oceans¹⁶ that are far from any possible point sources. Transport and deposition of PFAS is of concern because of the negative impacts of PFAS on ecosystems and human health.¹⁷⁻²¹

Here we focus on atmospheric transport of emerging PFAS through precipitation. PFAS removal by wet deposition depends on rain–air partition coefficients from the gas phase and from the particle phase.^{15,22} PFAS have been detected in precipitation from urban, rural, and remote sites around the world.⁹ Most studies have focused on deposition of perfluorinated carboxylic acids (PFCAs) and perfluorinated sulfonic acids (PFSAs) because historically these classes were in the most widespread use, particularly the C8 species PFOA (perfluorooctanoic acid) and PFOS (perfluorooctane sulfonic acid).^{15,22-30} Other species previously analyzed in wet deposition include perfluoroalkane sulfinic acids,³¹ perfluorinated ether carboxylic acids (PFECAs),^{32,33} perfluoroalkane sulfonamides,^{16,31,34,35} perfluoroalkane sulfonamido ethanols,³⁶ perfluoroalkyl sulfonamido acetic acids,^{31,35} fluorotelomer carboxylic acids (FTCAs),^{31,35,37,38} fluorotelomer sulfonic acids,³⁹ fluorotelomer unsaturated carboxylic acids (FTUCAs),^{16,31,34,35,37-39} and chlorinated PFAS.³⁹ The acronyms for PFAS classes are summarized in **Table S1**. In this

1
2
3 work, we use FTCAs to describe PFCAs with two F atom to H atom substitutions regardless of
4 the position of the H or whether the chain length is even or odd, and we use H-PFCAs
5 (hydrogen-substituted PFCAs) for a single F atom to H atom substitution, in keeping with the
6 notation in the FluoroMatch library.⁴⁰
7
8
9
10

11
12 PFAS are a diverse group of chemical compounds, encompassing thousands of structures,
13 and rapidly changing regulations are driving innovation among manufacturers.^{41,42} For example,
14 as restrictions on the use of PFOA and PFOS spread, shorter-chain species and species of other
15 functional classes, such as the C6 ether acid hexafluoropropylene oxide dimer acid (HFPO-DA,
16 trade name GenX) have become more prevalent.^{43–45} Based on total oxidizable precursor assays,
17 only a fraction of PFAS present in most environmental samples have been detected by targeted
18 approaches.^{39,46} With advances in high-resolution mass spectrometry (HR-MS), non-targeted
19 analysis (NTA) has become a powerful tool for solving the mystery of the unknown
20 fraction.^{44,47–49} NTA allows for the identification of unknown compounds without any *a priori*
21 assumptions about the sample.^{50,51} Formulas can be determined from accurate mass
22 measurements and isotopic distributions, and structures can be predicted from MS/MS
23 fragmentation patterns through comparison to experimental measurements or to *in silico*
24 calculations. Closely related to NTA is suspect screening, in which high-resolution mass spectra
25 are screened against extensive libraries. Among the many applications of HR-MS for PFAS
26 analysis in aqueous media, suspect screening and NTA have been used to identify emerging
27 PFAS in surface waters,^{52–56} industrial wastewater,^{57,58} municipal wastewater treatment
28 plants,^{59,60} and on particulate matter.^{61,62}
29
30
31
32
33
34
35
36
37
38
39
40
41
42
43
44
45
46
47
48
49
50

51 Comprehensive measurements by HR-MS facilitate source tracking of PFAS.^{63,64} The
52 isomeric profile of linear versus branched species acts as a sort of fingerprint for the compounds'
53
54
55
56
57
58
59
60

1
2
3 origins.⁶⁵ The manufacturing process of electrochemical fluorination (ECF) produces a mixture
4 of linear and branched products: 70-80% linear for PFOS, 80-85% linear for PFOA, and ~95%
5
6 linear for PFHxS (perfluorohexane sulfonic acid, C6), for example.⁶⁶ Telomerization, in contrast,
7
8 preserves the stereochemistry of the starting material (usually linear). Targeted mass
9
10 spectrometry with selective reaction monitoring can inaccurately measure the isomeric PFAS
11
12 profile if the chosen transitions do not capture all isomers and/or chromatographic separation is
13
14 insufficient. Determining whether the isomeric profile matches ECF is further complicated
15
16 because stereochemistry affects reactivity, acidity, water solubility, and partitioning.⁶⁵⁻⁷⁰
17
18 Measuring the isomeric profile of PFAS in a single compartment of the environment is often
19
20 insufficient to definitively assign sources.^{27,71-75} Nevertheless, isomeric profiles have been used
21
22 to determine that fluorotelomer alcohol (FTOH) degradation was the major source of PFAS
23
24 deposition to alpine lakes⁷⁶ and that a Norwegian lake was contaminated with PFAS from a
25
26 paper factory and not from a fire station⁷⁵. For atmospheric samples, branched PFAS isomers
27
28 have been quantified in precipitation from semirural and urban Canada;²⁷ in precipitation from
29
30 the urban centers of Beijing, Wuhan, and Stockholm;²⁴ in precipitation from islands off the
31
32 coasts of Sweden and Portugal;²⁴ and in particulate matter from urban centers in China.^{77,78} To
33
34 the best of our knowledge, there have been no studies of PFAS isomers in wet or dry deposition
35
36 samples in the United States.
37
38
39
40
41
42
43

44 Here we report the first applications of suspect screening and NTA to identify and semi-
45
46 quantitate PFAS in wet deposition. This work expands on our earlier targeted measurements of
47
48 the C2 and C4-C10 PFCAs, PFOS, and HFPO-DA in rainwater at six sites in the Ohio/Indiana
49
50 region of the central United States, with a reference site at approximately the same latitude in
51
52 Wyoming.³² The sampling network included a mix of rural, suburban, and semi-urban locations
53
54
55
56
57
58
59
60

1
2
3 with no known point sources near any of the collection sites. PFAS, including HFPO-DA, were
4 present in all samples from all sites in summer 2019. The concentrations at the Wooster, Ohio
5 site were significantly elevated compared to the other locations ($p < 0.05$). With new HR-MS
6 measurements for suspect screening and NTA, we seek to answer the question: What are we
7 missing with the narrow, targeted approach?
8
9

10
11
12
13
14
15 Our goals here are: (1) to identify and semi-quantitate emerging PFAS in precipitation
16 samples from the central United States, and (2) to assess sources and spatial trends of PFAS
17 through regional atmospheric transport. First, we used liquid chromatography quadrupole time-
18 of-flight mass spectrometry (LC-QTOF-MS) to analyze rainwater samples in MS-only mode to
19 screen mass-to-charge ratios against accurate mass lists from FluoroMatch⁴⁰ and NIST⁷⁹. We
20 then built a list of preferred ions for data-dependent acquisition of MS/MS spectra, and we
21 screened the resulting mass spectra against the FluoroMatch library. We supplemented suspect
22 screening with NTA using a CF₂ Kendrick mass defect analysis for homologous series of FTCAs
23 and H-substituted PFCAs,^{58,80} as well as cross-checks against characteristic fragmentation and
24 neutral loss patterns for PFAS.^{55,59,81} We semi-quantitated all identified PFAS with isotopically
25 labelled surrogates, and we conducted statistical analyses with Kruskal-Wallis tests, principal
26 component analysis (PCA), and Kendall's tau correlations. Finally, we used HYSPLIT^{82,83} to
27 model air mass back trajectories prior to precipitation events.
28
29
30
31
32
33
34
35
36
37
38
39
40
41
42
43
44
45

46 METHODS

47
48
49 **Reagents.** Isotopically labelled PFAS standards were obtained from Wellington (Guelph,
50 ON, Canada), as was the mixture of FTCA standards (2-perfluorohexyl ethanoic acid, 2-
51 perfluorooctyl ethanoic acid, and 2-perfluorodecyl ethanoic acid). Perfluoropropionic acid and
52
53
54
55
56
57
58
59
60

1
2
3 ammonium acetate (LC-MS grade) were obtained from Sigma Aldrich (St. Louis, MO, USA).

4
5 Solvents included LC-MS grade methanol (EMD Millipore) and Nanopure water (18.2 MΩ-cm).

6
7
8 **Sampling.** Figure S1 shows a map of the seven collection sites: Ashland, OH
9
10 (semiurban; 40.9°N, 82.3°W); Rockford, OH (rural; 40.7°N, 84.6°W); Shaker Heights, OH
11
12 (suburban; 41.5°N, 81.6°W); Whitestown, IN (suburban; 40.0°N, 86.4°W); Willoughby, OH
13
14 (suburban; 41.6°N, 81.4°W); Wooster, OH (industrial; 40.8°N, 81.9°W); and Jackson Hole, WY
15
16 (reference; 43.5°N, 110.8°W). The Wyoming site was selected because it is located at
17
18 approximately the same latitude at the Indiana/Ohio sites but at a distance of ~2,500 km. As
19
20 described in Pike et al.,³² rainwater was collected during precipitation events between May and
21
22 August of 2019. Samples were collected in high-density polyethylene (HDPE) tubs and stored in
23
24 HDPE bottles at 4 °C. At the Wooster site, a HDPE funnel and carboy were used in place of the
25
26 tub. Site blanks to check for contributions from dry deposition were collected at the beginning
27
28 and end of the campaign. On a day without rain, 1 L of Nanopure water was placed in the tub or
29
30 carboy and allowed to remain exposed to the atmosphere for 24-48 hours. A ride-along blank
31
32 was also prepared for the Whitestown site by shipping a 1-L bottle of Nanopure water along with
33
34 the sample bottles. Sample analysis was conducted in Wooster, OH. **Table S2** in the Supporting
35
36 Information lists the number of samples and blanks from each site.
37
38
39
40
41

42 **Sample Preparation.** Full details of the sample preparation procedure are given
43
44 elsewhere.^{31,32} Briefly, samples were spiked with 5.6 ng of each of the following isotopically
45
46 labelled standards: perfluoro-*n*-[1,2,3,4-¹³C₄]butanoic acid (M4PFBA); perfluoro-*n*-[3,4,5-
47
48 ¹³C₃]pentanoic acid (M3PFPeA); perfluoro-*n*-[1,2-¹³C₂]hexanoic acid (M2PFHxA); perfluoro-*n*-
49
50 [1,2,3,4-¹³C₄]heptanoic acid (M4PFHpA); perfluoro-*n*-[1,2,3,4-¹³C₄]octanoic acid (M4PFOA);
51
52 perfluoro-*n*-[1,2,3,4,5-¹³C₅]nonanoic acid (M5PFNA); perfluoro-*n*-[1,2-¹³C₂]decanoic acid
53
54
55
56
57
58
59
60

1
2
3 (MPFDA); sodium perfluoro-1-[2,3,4-¹³C₃]butanesulfonate (M3PFBS); sodium perfluoro-1-
4 hexane[¹⁸O₂] sulfonate (MPFHxS); sodium perfluoro-1-[1,2,3,4-¹³C₄]octanesulfonate
5
6 (M4PFOS); and 2,3,3,3-tetrafluoro-2-(1,1,2,2,3,3,3-heptafluoropropoxy)-¹³C₃-propanoic acid
7
8 (M3HFPO-DA). Each sample, typically between 500 mL to 1 L, was concentrated by solid-
9
10 phase extraction (SPE) with Oasis WAX cartridges (250 mg, Waters). SPE cartridges were
11
12 conditioned with 4 mL of methanol + 0.1% ammonia, 4 mL of methanol, and 5 mL of Nanopure
13
14 water. The sample was applied, and cartridges were rinsed with 5 mL of Nanopure water. A first
15
16 elution step was conducted with 4 mL of methanol to collect neutral PFAS, which were not
17
18 analyzed here. A second elution step was conducted with 4 mL of methanol + 0.1% ammonia to
19
20 collect the eluate analyzed in this work. Eluates were evaporated to dryness using a homebuilt,
21
22 Teflon-free nitrogen evaporator, and samples were reconstituted in 250 μL of methanol. A
23
24 pooled sample was prepared by combining 10 μL aliquots of all the reconstituted sample extracts
25
26 including blanks.

27
28
29
30
31
32
33 ***Instrumentation.*** Samples were analyzed with an Agilent 1260 Infinity II liquid
34
35 chromatograph and Agilent 6545 quadrupole time-of-flight mass spectrometer. A C18 column
36
37 was used for the chromatographic separation, and negative electrospray was used for ionization.
38
39 Data were first collected in MS-only mode, and all samples were subsequently re-analyzed
40
41 through data-dependent MS/MS acquisition with a preferred ions list. Full method details for
42
43 chromatography and mass spectrometry are provided in **Table S3**.

44
45
46
47 ***Data Analysis.*** The Agilent MassHunter 10.0 software suite and the open-source
48
49 software MS-DIAL (version 4.60)⁸⁴ were used for data processing. The FluoroMatch PFAS
50
51 library was used for suspect screening.⁴⁰ MS-DIAL parameters are summarized in **Table S4**.

1
2
3 Strategies for feature reduction, suspect screening, and non-targeted analysis are discussed in the
4
5 Results section.
6

7
8 ***Semiquantitation.*** Concentrations of emerging PFAS were estimated by scaling the peak
9
10 area of the analyte against the peak area of the isotopically labelled surrogate closest in retention
11
12 time.⁸⁵ Because surrogates were added prior to solid-phase extraction, their concentrations in the
13
14 samples are known exactly.³² This semi-quantitative calculation introduces appreciable
15
16 uncertainty when the analyte and the surrogate are not structurally similar and their relative
17
18 extraction efficiencies, ionization efficiencies, etc. are unknown. Nevertheless, concentration
19
20 ratios from one sample to another remain meaningful with this scaling method since the samples
21
22 are similar in composition.
23
24

25
26 Next, concentrations (mass per volume) were converted to estimated deposition fluxes
27
28 (mass per unit area) using precipitation amounts from the nearest National Weather Service
29
30 station.⁸⁶ The deposition flux F in ng m^{-2} is given by:
31
32

$$33 \quad F = 1000 \times C \times d \quad (1)$$

34
35 where C is the concentration in ng L^{-1} , d is the rainfall amount in meters, and 1000 is a
36
37 conversion factor between m^3 and L. Calculating flux rather than concentration is necessary to
38
39 account for washout and scavenging of PFAS at the start of a precipitation event.¹⁶ Further
40
41 discussion of the uncertainties in deposition flux can be found in Pike et al.³²
42
43

44
45 ***QA/QC.*** The Non-Targeted Analysis (NTA) Study Reporting Tool (SRT) was used in
46
47 designing QA/QC measures and preparing this manuscript.^{87,88} Isotopically labeled PFAS
48
49 surrogates were added to precipitation samples prior to solid-phase extraction, as described
50
51 previously³² (see **Table S5** and Sample Preparation section for list of surrogates). Recoveries and
52
53
54
55
56
57
58
59
60

1
2
3 analysis of blanks were outlined previously and shown to be acceptable; results are summarized
4
5
6
7 in **Tables S6 and S7**.³² All precipitation extracts were analyzed by LC-QTOF in random order on
8
9
10 a contiguous worklist. Prior to measurement, a pooled sample containing 10 μL of each
11
12
13 precipitation extract sample (including site blanks) was prepared. The pooled sample, an
14
15
16 instrument blank, and a standard mixture containing 5 ng mL^{-1} of each PFAS (**Table S8**) were
17
18
19 measured after every eighth sample in the worklist. The standard deviation of the retention time
20
21
22 and relative standard deviation of peak areas are listed in **Table S8** for the standard and **Table S9**
23
24
25 for the pooled sample. Standards of perfluoropropionic acid and fluorotelomer carboxylic acids
26
27
28 were analyzed separately using the same method as samples. Upon re-analysis using data-
29
30
31 dependent MS/MS acquisition, the same worklist (with inclusion of instrument blanks, pooled
32
33
34 sample replicates, and instrument performance check standards) was used. Inclusion of a feature
35
36
37 as a suspect PFAS required the peak area to be statistically higher than peak areas found in
38
39
40 instrument and site blanks. Concentrations in the site blanks were not subtracted from
41
42
43 concentrations in the samples. Instead, compounds that did not have concentrations significantly
44
45
46 higher in the samples than in the blanks (by a one-sided *t*-test, $p < 0.05$) were removed from
47
48
49 further analysis.
50
51
52
53
54
55
56
57
58
59
60

1
2
3 **Statistics.** Analyses and visualization were carried out using RStudio (version 4.1.2).⁸⁹
4
5 Non-parametric tests were selected due to the data not following a normal distribution. Statistical
6
7 analyses performed include Kruskal-Wallis tests, pairwise Wilcoxon Rank Sum post-hoc tests,
8
9 Kendall's tau correlations, and principal component analysis (PCA). For all statistical tests,
10
11 values below the detection limit were replaced with a value of zero. Results with a *p*-value less
12
13 than 0.05 were considered significant.
14
15

16
17 **HYSPLIT.** The Hybrid Single-Particle Lagrangian Integrated Trajectory model
18
19 (HYSPLIT version 5) was used to calculate air mass back trajectories for each rain event.⁸³
20
21 Meteorological data came from the National Centers for Environmental Prediction/National
22
23 Center for Atmospheric Research (NCEP/NCAR) Reanalysis Project at $2.5^\circ \times 2.5^\circ$ spatial
24
25 resolution and 6-hour temporal resolution.⁹⁰ From the origin at the collection site, trajectories at
26
27 500, 1000, and 3000 m above ground level were traced backwards six days with a new trajectory
28
29 added every four hours.
30
31

32 33 34 35 **RESULTS AND DISCUSSION**

36 37 **PFAS Identification**

38
39
40 All precipitation standards and a pooled sample were measured by LC-QTOF in MS-only
41
42 mode. The data as a collective were peak-aligned and processed with MS-DIAL (version 4.60)⁸⁴
43
44 using a FluoroMatch library (version 2.431)^{40,91} to find molecular features that may be attributed
45
46 to PFAS. The initial screen of the MS-only data identified 10,594 potential PFAS features, the
47
48 majority of which had negative mass defects. High-quality features were identified by selecting
49
50
51
52
53
54
55
56
57
58
59
60

1
2
3 those with the following five criteria filtered in the order listed: (i) signal-to-noise (S/N) ratio
4
5
6
7 >200, (ii) quality scores >90%, (iii) peak heights >15,000 in the pooled sample, (iv) formulas
8
9
10 that contained only F as a halogen, (v) and a putative identification determined to be reasonable
11
12
13 based on retention time compared to standards (within 0.2 min). Relatively high data quality
14
15
16
17 thresholds were applied in order to provide certainty to the identifications since there are few
18
19
20 studies of emerging PFAS in precipitation. Application of the criteria resulted in 96 features. The
21
22
23
24 96 high-quality features were then added as preferred ions in a MS/MS re-analysis of the
25
26
27 samples by LC-QTOF in the Auto-MS/MS mode of Agilent MassHunter Acquisition 10.0
28
29
30 software. Data were then analyzed using the FluoroMatch MS/MS library via MS-DIAL,
31
32
33
34 resulting in 979 features. The number was further reduced to 74 high-quality features based on
35
36
37 S/N and retention time criteria. The 74 high-quality features were further assessed by verifying
38
39
40 fragment ion matches found in MS/MS library spectra. Since most of the 74 compounds differed
41
42
43 only by chain length, Kendrick mass defect plots were used to validate the assignments (**Figure**
44
45
46
47 **S2**). Many of the 74 compounds were H-substituted perfluorocarboxylates of various chain
48
49
50 lengths, eluted stepwise chromatographically within the homologous series (**Figure S3**).
51
52
53
54 Application of all the criteria above resulted in the identification of 24 emerging PFAS
55
56
57
58
59
60

1
2
3 compounds with confidence levels of 3a or above according to the scale defined by Charbonnet
4
5
6 et al.⁹² See **Table 1** for the list of emerging PFAS and **Appendix A** of the SI for full data. As a
7
8
9
10 final check, the MS-only data set was re-screened using the NIST PFAS suspect list⁷⁹ and
11
12
13 Agilent MassHunter Qualitative Analysis (version 10.0). The NIST suspect screening in
14
15
16 MassHunter identified a total of 3,935 features, including the 74 high-quality features determined
17
18
19 via the analysis through MS-DIAL using the FluoroMatch library. It is noted that the stringency
20
21
22 of the data analysis likely excluded low-abundance features. Further searches for additional
23
24
25
26
27 emerging PFAS can be done in the future, and data are available upon request.
28
29

30 Reference standards were commercially available for compounds **2**, perfluoropropionic
31
32 acid (PFPrA); **11**, 2-perfluorohexyl ethanoic acid (6:2 FTCA); **17**, 2-perfluorooctyl ethanoic acid
33
34 (8:2 FTCA); and **21**, 2-perfluorodecyl ethanoic acid (10:2 FTCA), according to the numbering
35
36
37 scheme in **Table 1**. The standards were analyzed with the same LC-QTOF method used for the
38
39
40 samples in both MS-only and MS/MS modes. Retention times matched the presumed linear
41
42
43 version of the features in the samples, allowing a level 1 confidence according to the scale by
44
45
46 Charbonnet et al.⁹² Interestingly, significant in-source fragmentation was observed for the
47
48
49 telomer acids, especially for the reference standards, which consisted of only the linear isomers.
50
51
52
53
54
55
56
57
58
59
60

1
2
3
4 Fragmentation led to the loss of $\text{CH}_2\text{O}_2\text{F}_2$ for all FTCA standards. Overall, there is high
5
6
7 confidence in the identity of the compounds listed in **Table 1** based on signal strength, mass
8
9
10 defect score, matching to an MS/MS library, identification by both FluoroMatch and NIST
11
12
13 databases, and retention times predicted for homologous series.
14
15

16
17 Additional emerging PFAS were potentially identified out of the 74 high-quality features
18
19
20 measured in MS/MS mode. These features had confidence levels below 3a as they lacked a
21
22
23 match to a library spectrum, had too few fragments, or had a S/N ratio <200 . Compounds with
24
25
26 S/N > 100 and retention times that are reasonable based on retention times of standards ($n = 22$)
27
28
29 are listed in **Table S10**.
30
31
32
33
34
35
36
37
38
39
40
41
42
43
44
45
46
47
48
49
50
51
52
53
54
55
56
57
58
59
60

Compound	Structure (linear isomer)	Formula	RT	Ref Mass	m/z	Δ ppm	MS/MS 1	MS/MS 2	MS/MS 3	Surrogate	Confidence
(1) 2:2 FT carboxylic acid		C ₄ H ₃ F ₅ O ₂	3.21	176.9981	176.9980	0.08	92.9950			MPFPeA	2a
(2) Perfluoropropionic acid		C ₃ HF ₅ O ₂	3.55	162.9824	162.9828	0.40	118.9933			MPFPeA	1a
(3) 3:2 FT carboxylic acid (n=3)		C ₅ H ₃ F ₇ O ₂	4.97	226.9949	226.9954	0.56	92.9958	142.9930		MPFPeA	2b
(4) PFCA-perfluoroalkyl- Hsubstituted-1DB (n=2)		C ₅ H ₂ F ₆ O ₂	5.89	206.9886	206.9880	0.57	92.9958	142.9940		MPFPeA	2a
(5) Perfluoropropane sulfonate		C ₃ HF ₇ O ₃ S	6.83	248.9462	248.9460	0.21	79.9576	98.9561		MPFBS	2b
(6) H-substituted perfluoroalkyl dioic acid (n=7)		C ₁₀ H ₃ F ₁₅ O ₄	6.83	470.9719	470.9730	1.16	192.9895	292.9837	342.9815	MPFDA	2a
(7) unsaturated-ether-PFCA (n=2)		C ₇ HF ₁₁ O ₃	7.47	340.9677	340.9678	0.06	118.9935			MPFHpA	2c
(8) H-substituted perfluoroalkyl dioic acid(n=8)		C ₁₁ H ₃ F ₁₇ O ₄	9.14	520.9687	520.9692	0.49	242.9871			MPFDA	2b
(9) OPFC-perfluoroalkyl sulfate (n=4)		C ₈ H ₁₀ F ₈ O ₄ S	10.53	353.0099	353.0032	6.69	204.9903			MPFOS	3a
(10) H-substituted- unsaturated ether - PFCA (n=7)		C ₁₂ H ₄ F ₁₈ O ₃	11.42	536.9800	536.9777	2.32	192.9889	242.9871	292.9826	MPFDA	3a
(11) 6:2 FT carboxylic acid (n=6)		C ₈ H ₃ F ₁₃ O ₂	11.66	376.9853	376.9846	0.67	92.9959	242.9886	292.9831	MPFOA	1a
(12) H-substituted-PFCA (n=5)		C ₇ H ₂ F ₁₂ O ₂	11.98	344.9790	344.9790	0.00	118.9902	280.9828		MPFHpA	2a
(13) 7:2 FT carboxylic acid (n=7)		C ₉ H ₃ F ₁₅ O ₂	12.36	426.9821	426.9836	1.55	192.9895	342.9824		MPFNA	2a
(14) H-substituted PFCA (n=6)		C ₈ H ₂ F ₁₄ O ₂	13.30	394.9759	394.9772	1.34	118.9929	330.9800		MPFOA	2a
(15) PFCA-perfluoroalkyl- Hsubstituted-1DB (n=5)		C ₈ H ₂ F ₁₂ O ₂	13.22	356.9793	356.9787	0.33	92.9958	142.9926	292.9816	MPFOA	2c
(16) Perfluoroalkyl sulfonate (n=7)		C ₇ HF ₁₅ O ₃ S	13.90	448.9334	448.9358	2.41	79.9576	98.9563	118.9931	MPFOS	2c
(17) 8:2 FT carboxylic acid (n=8)		C ₁₀ H ₃ F ₁₇ O ₂	14.258	476.9789	476.9776	1.25	118.9902	242.9870	392.9763	MPFDA	1a
(18) H-substituted-PFCA (n=7)		C ₉ H ₂ F ₁₆ O ₂	14.65	444.9727	444.9722	0.49	118.9932	380.9774		MPFNA	2a
(19) 9:2 FT carboxylic acid (n=9)		C ₁₁ H ₃ F ₁₉ O ₂	15.15	526.9757	526.9748	0.92	118.9932	292.9828	442.9734	MPFDA	2a
(20) H-substituted-PFCA (n=8)		C ₁₀ H ₂ F ₁₈ O ₂	15.54	494.9694	494.9684	1.04	118.9932	168.9889	430.9732	MPFDA	2a
(21) 10:2 FT carboxylic acid		C ₁₂ H ₃ F ₂₁ O ₂	16.21	576.9725	576.972	0.73	118.9932	242.9860	492.9703	MPFDA	1a
(22) H-substituted-PFCA (n=9)		C ₁₁ H ₂ F ₂₀ O ₂	16.76	544.9662	544.9664	0.18	118.9932	168.9890	480.9674	MPFDA	2a
(23) 11:2 FT carboxylic acid		C ₁₃ H ₃ F ₂₃ O ₂	17.17	626.9693	626.9685	0.79	242.9880	342.9824	542.9716	MPFDA	2a
(24) H-substituted-PFCA (n=10)		C ₁₂ H ₂ F ₂₂ O ₂	17.89	594.9631	594.9635	0.43	118.9928	168.9895	268.9836	MPFDA	2a

Table 1: Emerging PFAS analytes identified by non-targeted analysis, mass spectral data, and confidence levels. 15

1
2
3
4 Most of the 24 emerging compounds identified with high confidence (**Table 1**) are H-
5
6
7 substituted fluorinated carboxylic acids similar in chain length (C4-C12) to PFAS compounds on
8
9
10 the EPA list. Incomplete fluorination and presence of odd chain lengths (ex. **13**, 7:2 FTCA)
11
12
13 suggest the compounds were manufactured by electrochemical fluorination.⁹³ Curiously, many of
14
15
16 the compounds had substantial amounts of branched isomers (see below), especially in the
17
18
19 Wooster samples. The emerging compounds are different from aqueous film forming foam
20
21
22 compositions reported in the literature.^{31,94-96} FTCAs have been reported in precipitation
23
24
25 elsewhere,^{35,38,39} but to the best of our knowledge, this study marks the first detection in
26
27
28 rainwater of H-PFCAs with a single F atom to H atom substitution. Furthermore, we present the
29
30
31 first report of such highly branched FTCAs and H-PFCAs, so little is known about possible
32
33
34 sources. Other emerging compounds identified with high confidence included PFAS with two
35
36
37 carboxylate end groups and other compounds with H-substituted perfluorosulfonates. The
38
39
40 additional 22 emerging PFAS compounds with lower confidence (**Table S10**) showed a more
41
42
43 diverse set of polar functional groups including sulfonates, thioether acetic acids, sulfonamides,
44
45
46 and amines. It should be noted that most of the 22 compounds were at lower concentrations
47
48
49
50
51
52
53
54
55
56
57
58
59
60

1
2
3 compared to the compounds listed in **Table 1**. However, if the identifications are accurate, these
4
5
6
7 data indicate that a wide diversity of PFAS was found in the sampled precipitation.
8
9

10 The presence of the emerging PFAS compounds in precipitation may be linked to the
11
12 manufacturing process and to volatility, which influences atmospheric mixing ratios. Vapor
13
14 pressure increases as the chain length decreases and as the pK_a of the acid group increases,
15
16
17 allowing the neutral, more volatile species to form at a lower pH. Substitution of H for F near the
18
19
20 carboxylate head group in PFCAs reduces electron induction effects and raises the pK_a by ~2-3
21
22
23
24 units.⁹⁷ It may be that H-PFCAs are optimal for atmospheric deposition because they possess a
25
26
27
28
29
30
31 pK_a high enough to promote volatilization of the neutral protonated form and they are also acidic
32
33
34 enough to promote dissolution in aqueous aerosol particles and cloud droplets.
35
36
37
38
39

40 **Fluorocarbon Chain Length and Branched Isomers**

41
42 Polyfluorinated carboxylic acids were the most commonly detected emerging PFAS in
43
44 precipitation samples, particularly in the Wooster location. Compounds with even-length
45
46
47 fluoroalkyl chains such as **11**, **17**, **21** (6:2 FTCA, 8:2 FTCA, and 10:2 FTCA, **Table 1**) are
48
49
50
51 typically produced by telomerization, which due to the synthesis mechanism, results in linear
52
53
54
55
56
57
58
59
60

1
2
3
4 carbon chains with even numbers of fluorinated carbon groups.^{93,98} Similarly, the oxidation of
5
6
7 fluorotelomer alcohols in the environment also results in the same even-numbered chain length
8
9
10 speciation of PFCAs.⁹⁹ However, we found that precipitation samples had substantial amounts of
11
12
13 odd chain length PFCAs, for example, compound **13**, 7:2 FTCA. Such findings are not indicative
14
15
16 of an even chain length series that would be predicted for PFAS produced by
17
18
19 fluorotelomerization. Odd chain length compounds were often at the same order of magnitude in
20
21
22 concentration as the even chain length PFAS in the rainwater samples. For example, the relative
23
24
25 ratios of the estimated concentrations of 6:2, 7:2, 8:2, 9:2, and 10:2 FTCA for the 5 June 2019
26
27
28 Wooster sample were 2.6 : 5.0 : 3.5 : 2.2 : 1.0, respectively. High concentrations of odd chain
29
30
31 length compounds were consistent for samples at the Wooster location, with 7:2 FTCA
32
33
34 sometimes having a concentration similar to even chain PFAS. The presence of odd chain
35
36
37 lengths of PFAS may indicate other unknown local sources near the Wooster sampling site that
38
39
40 contribute besides direct emission and deposition of fluorotelomer-derived products from the
41
42
43 atmosphere.
44
45
46
47
48
49

50 Another notable observation was the large number of chromatographically distinct peaks
51
52
53 observed for the emerging PFAS. For example, the extracted ion chromatogram (EIC) of the
54
55
56
57
58
59
60

1
2
3
4 376.9846 m/z ion corresponding to 6:2 FTCA has many peaks distributed across the retention
5
6
7 time window of 10.5-13.2 min (**Figure 1**). The peaks were attributed to branched isomers,¹⁰⁰
8
9
10 which typically have shorter retention times due to lower affinity of branched chains to the C18
11
12
13 stationary phase because steric effects reduce lipophilicity.^{101,102} Interestingly, there were at least
14
15
16
17 11 chromatographic peaks for 6:2 FTCA, which may be due to both variations in the degree of
18
19
20 branching and the position of the C-H groups relative to the carboxylate end group. The
21
22
23 commercial standard for 6:2 FTCA (alternatively named 2-perfluorohexyl ethanoic acid) is the
24
25
26
27 linear form, which can be used to verify the straight-chain isomer. Based upon the relative peak
28
29
30 areas of the linear and branched forms, >70% of the 376.9846 m/z ion feature in the pooled
31
32
33
34 sample was present as putative branched isomers. This high degree of branching is
35
36
37 uncharacteristic of PFAS manufactured by telomerization, where linear straight chain
38
39
40 compounds are the predominant isoforms, nor does the profile match what is typically observed
41
42
43
44 for PFCAs produced by ECF.⁶⁶ It was observed that the branched isomers in the precipitation
45
46
47 samples exhibited less in-source fragmentation compared to the linear standards. Gas-phase
48
49
50 dimerization was observed in the mass spectra of the linear FTCA standards, but was generally
51
52
53
54 absent in the spectra of the putative branched features. We note that when calculating the amount
55
56
57
58
59
60

1
2
3 of PFAS, the sum of peak areas for both the linear and branched forms was used in semi-
4
5
6
7 quantification.
8
9

10 The peaks of the m/z 376.9846 ion elute across a two-minute retention time window,
11
12
13 which is a fairly broad elution profile. Nevertheless, we conclude that the peaks are isomers
14
15
16 because they correspond to a single exact mass. Such a wide range is possible given that
17
18
19 Pellizzaro et al.¹⁰² determined that a C8 perfluorinated PFAS has 89 potential congeners.
20
21
22
23 Substitution by H for one or more F atoms leads to substantially more congeners and structural
24
25
26 diversity. One of the reasons for the substantial variation in retention times is the slowly
27
28
29 changing solvent gradient used that is two times longer compared to previous reports.¹⁰³ The
30
31
32
33 chemical interactions between a PFAS analyte and a non-polar stationary phase are not widely
34
35
36 understood. The substitution of an H atom to various isomers appears to lead to substantial
37
38
39 changes in affinity to the C18 stationary phase, potentially due to differences in polarity in parts
40
41
42
43 of the PFAS structure or to steric effects. The unique chromatographic behavior of H-substituted
44
45
46 emerging PFAS could be further studied in the future to better understand the properties of this
47
48
49
50 class of molecules.
51
52
53
54
55
56
57
58
59
60

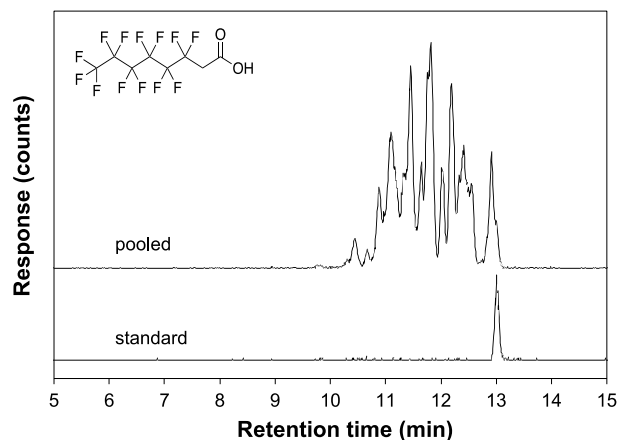


Figure 1. Extracted ion chromatograms of m/z 376.9846 corresponding to compound 14 (6:2 FTCA) of the pooled sample (top) and the analytical standard (bottom) comprised of the linear isomer.

All of the H-substituted PFCA compounds identified in **Table 1** showed multi-peak EICs characteristic of substantial amounts of branched isomers (Supplemental Information, Appendix A). The distributions of the chromatographic peaks (and, by extension, the isomeric branching profiles) were evaluated with respect to sampling location and date. The chromatographic profile at Wooster was unique compared to other sites, where the EICs exhibited less overall abundance and fewer peaks at earlier retention times. For instance, compound 14, a H-substituted analogue of PFOA ($m/z = 394.9772$) had five distinct peaks, whereas only the peaks with the shortest retention times were present in the chromatograms from samples at other sites (**Figure 2**). At

1
2
3
4 Wooster, the presumably branched isomer with the longer retention time dominated in terms of
5
6
7 peak area. The isomeric profiles at Wooster in comparison to the profiles at the other sampling
8
9
10 sites were consistent regardless of date, implying that location was the dominant factor
11
12
13 controlling PFAS profiles. We hypothesize that Wooster is located in close proximity to a unique
14
15
16 PFAS point source at the time of sampling, whereas the profiles at the other locations are more
17
18
19 indicative of an average PFAS background. Moreover, background levels of H-substituted
20
21
22
23 PFCAs appear more branched than the perfluorinated species. It is unknown why the more polar
24
25
26 isomers are the predominant forms with high abundance in the diffuse regional background,
27
28
29 perhaps due to long-term persistence and/or long-range transport. Further studies correlating the
30
31
32
33 physical properties of emerging isomeric-rich PFAS and their fate and transport could be
34
35
36
37 informative.¹⁰⁴
38
39
40
41
42
43
44
45
46
47
48
49
50
51
52
53
54
55
56
57
58
59
60

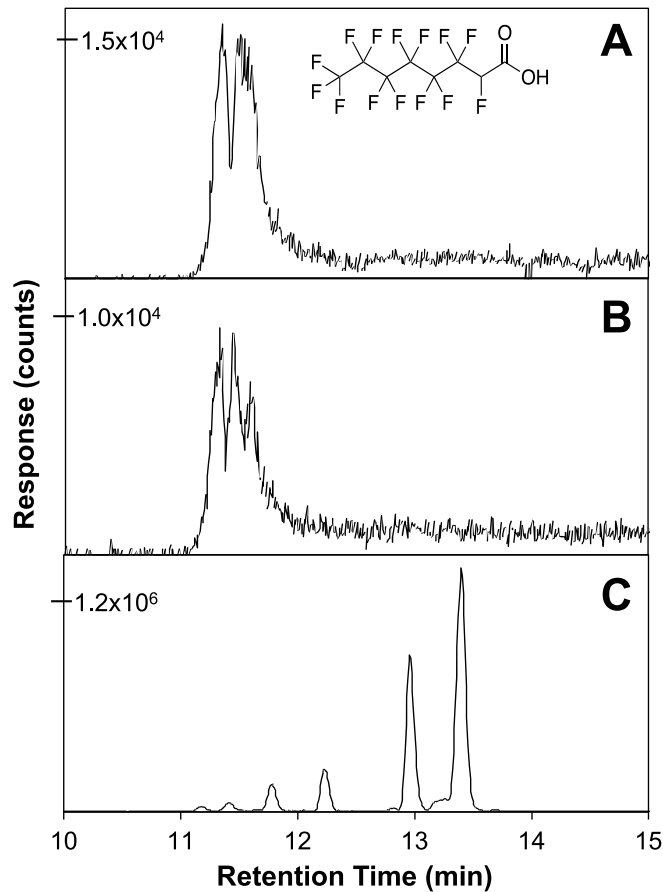


Figure 2. Extracted ion chromatograms for m/z 394.9759 corresponding to compound 11, H-substituted PFCA from **A**, Ashland, OH; **B**, Rockford, OH; **C**, Wooster OH.

EPA-list PFAS compounds showed much less branching compared to the emerging PFAS. For example, the branched fractions of PFOA (C8 perfluorinated carboxylic acid) and PFHxS (C6 perfluorinated sulfonic acid) comprised <15% of the overall peak area (see **Figures S4 and S5**). The limited degree of PFOA branching is consistent with other literature reports testing precipitation samples.^{24,27} Overall, the polyfluoro (H-substituted) compounds in our

1
2
3 rainwater samples consisted primarily of branched isomers, whereas the perfluorinated
4
5
6
7 compounds were primarily found as linear isomers. It is unknown if the differences in profile are
8
9
10 due to source variation, to distinct transformation pathways, or to changes in physical properties
11
12
13 (e.g., pK_a) that alter partition ratios for the different classes of PFAS. However, these data
14
15
16
17 suggest that further work is sorely needed to better model the occurrence, fate, and transport of
18
19
20 emerging PFAS.⁴¹
21
22

23
24 Both the high degree of branching among FTCA isomers and the presence of FTCAs
25
26
27 with odd-numbered chain lengths in precipitation from Wooster suggest a unique localized point
28
29
30 source during the sampling time period.¹⁰⁵ Thermal degradation of PFAS source compounds
31
32
33
34 could explain the unique range of compounds detected at Wooster; however, recent literature
35
36
37 reviews note that the thermal transformation processes of PFAS are poorly understood,^{106,107} and
38
39
40 data have indicated that PFAS destruction efficiencies depend upon structure, combustion
41
42
43
44 chemistry, temperature, and operational conditions, such the presence or absence of
45
46
47 oxygen.^{108,109} Xiao et al.¹¹⁰ studied the thermal stability and decomposition kinetics of PFAS
48
49
50 from spent granular activated carbon during thermal regeneration. Interestingly, a PFOA thermal
51
52
53
54 degradation intermediate with a precursor m/z of 395 and a fragment m/z of 119 was detected by
55
56
57
58
59
60

1
2
3
4 low-resolution mass spectrometry.¹¹⁰ This species could correspond to compound **14** (**Table 1**)
5
6
7 found in our precipitation samples. It is critical to note that the source of additional PFAS
8
9
10 detected at the Wooster site is unknown. However, the differences in emerging PFAS seen at
11
12
13
14 Wooster indicate that PFAS can vary at the sub-regional scale.
15
16
17
18
19

20 **Concentrations and Fluxes of PFAS in Rainwater**

21
22 Concentrations and deposition fluxes for the newly identified PFAS are given in **Tables**
23
24 **S11 and S12**, respectively, for the precipitation samples at each site. Concentrations in the
25
26 blanks are given in **Table S13**. The sum of all PFAS (Σ_{PFAS}) includes the ten PFAS quantified in
27
28 Pike et al.³² and the 22 PFAS semi-quantified in this work. (Compounds **22** and **24** from **Table 1**
29
30 are excluded from the analysis because of their high presence in method blanks.) We refer to
31
32 compounds as emerging if they do not appear in EPA Method 533¹¹¹ and/or 537.1¹¹².
33
34
35

36 The most notable result from the semi-quantitative analysis is the anomalously high level
37
38 of PFAS in rainwater from Wooster. To the best of our knowledge, H-PFCAs have never before
39
40 been reported in precipitation, and the median concentrations and fluxes of $\Sigma_{\text{H-PFCAs}}$ are 782 ng
41
42 L⁻¹ and 4.3×10^4 ng m⁻², respectively, in Wooster. We also report the first published
43
44 measurements of 8:2 FTCA, 10:2 FTCA, and 6:2 FTUCA in rainwater anywhere since 2010³⁵
45
46 (and in the United States since 1999)³⁸. Concentrations of these species in Ashland, Shaker
47
48 Heights, Willoughby, and Rockford are on the same order as what has been seen
49
50 elsewhere.^{31,35,37,38} In contrast, concentrations in Wooster are higher by 1-2 orders of magnitude,
51
52
53 as shown in **Figure S6**. The exceptionally high PFAS levels in rainwater from Wooster, coupled
54
55
56
57
58
59
60

1
2
3 with the unique profiles discussed above, imply that a point source is likely present in the
4 immediate vicinity of the sampling site. A previous study of the influence of point sources on
5 PFAS deposition was conducted by Barton et al.,²² who measured PFOA in rainwater collected
6 in 2005 near a manufacturing plant that was actively using ammonium perfluorooctanoate. The
7 authors found PFOA concentrations of 1660 ng L⁻¹ in rainwater collected at the manufacturing
8 site, but the concentrations dropped to ~10 ng L⁻¹ at a distance of just 1 mile from the plant.²²
9
10 The median Σ_{PFAS} concentration in our Wooster samples was 4450 ng L⁻¹, on the same order as
11 the concentration of PFOA observed by Barton et al.²² directly at the point source. The
12 difference in PFAS levels at Wooster relative to the other Ohio/Indiana sites in our 2019
13 measurement campaign highlights the fact that sub-regional variations in PFAS deposition
14 profiles are possible, presumably due to localized sources.
15
16
17
18
19
20
21
22
23
24
25
26
27

28 Regulations and restrictions surrounding PFAS use have certainly expanded since the
29 2005 measurements by Barton et al.²² We no longer observe parts per billion levels of PFOA in
30 rainwater samples, but we do see parts per billion levels of emerging PFAS in rainwater. Indeed,
31 **Figure S6** shows that FTCA and FTUCA levels are even higher now than they were in prior
32 decades. Although the absolute concentrations and fluxes in **Tables S11-S12** are approximate
33 because of the limitations of semi-quantitation, the values are still alarmingly high. In 2022, the
34 U.S. EPA updated its lifetime health advisories for drinking water to just 0.004 ng L⁻¹ PFOA,
35 0.02 ng L⁻¹ PFOS, 0.01 ng L⁻¹ GenX (HFPO-DA), and 2000 ng L⁻¹ PFBS (C4 sulfonic acid).¹¹³
36
37 With a maximum Σ_{PFAS} concentration of 16,400 ng L⁻¹ in rainwater from Wooster, our results
38 show that these advisories, while ambitious, are likely insufficient to mitigate PFAS intake,
39 especially given the diversity of emerging PFAS now present in the environment.
40
41
42
43
44
45
46
47
48
49
50
51
52
53
54
55
56
57
58
59
60

Statistical Testing

Statistical testing was carried out to address whether PFAS profiles in Wooster were significantly different from profiles elsewhere with reference to class, functional group, or chain length. Comparisons between sites and PFAS class build on our earlier statistical analysis,³² which was limited to a subset of 10 PFAS (C2 and C4-C10 PFCAs, PFOS, and HFPO-DA) in precipitation. All statistical tests herein for samples compared estimated deposition fluxes instead of concentrations to remove influences of washout and scavenging, which cause PFAS concentrations to decrease over the course of a precipitation event.¹⁶ We note that the estimated deposition fluxes integrate both wet and dry deposition over each sampling period, but dry deposition appeared to contribute a minor fraction of PFAS according to the site blanks in **Table S13**. (Samples and blanks were compared using concentrations from **Table S13** rather than fluxes because the method of calculating deposition fluxes through equation 1 is restricted to precipitation events and cannot be extended to blanks.) Finally, we acknowledge that the estimated deposition fluxes bear inherent uncertainty because of the semiquantitative nature of suspect screening and non-targeted analysis. Nevertheless, Kruskal-Wallis tests, Kendall's tau correlations, and PCA can provide insight into trends within the data set.

Overall deposition flux. A Kruskal-Wallis test was used to compare estimated deposition fluxes of all PFAS across sampling sites (**Figure 3**). As anticipated, deposition of PFAS in Wooster was significantly different from deposition at most other sampling sites. All other sites showed no statistical difference in estimated deposition fluxes. The significantly greater flux in Wooster suggests that a local point of PFAS contamination is likely present.

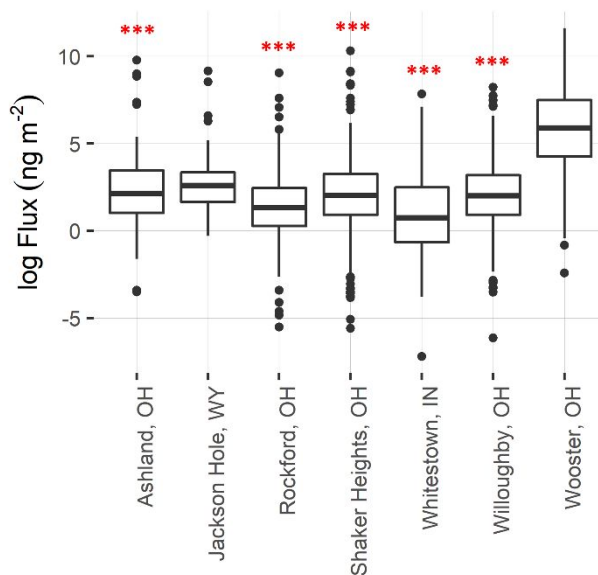


Figure 3. Boxplot comparing the logarithm of the estimated PFAS deposition fluxes (in ng m^{-2}) of each compound and sampling date across each site. Red asterisks denote sampling sites with significantly different ($p < 0.05$) estimated deposition fluxes from Wooster, OH. Black points indicate outliers for each sampling site.

EPA monitoring status. In this work, suspect screening and a non-targeted approach allowed for 23 emerging PFAS to be identified with high confidence (**Table 1**, excluding EPA-monitored compound **16**). **Figure 4** compares the estimated deposition flux of EPA-monitored PFAS and emerging PFAS at each site. Shaker Heights, Willoughby, and Wooster displayed significantly different estimated deposition fluxes when comparing EPA-monitored and emerging PFAS according to a Kruskal-Wallis test (**Table S14**). At each site, estimated deposition fluxes of emerging PFAS exceeded those of EPA-monitored PFAS. Indeed, our results likely underestimate the PFAS fraction in rainwater comprised by emerging compounds because we did not quantify the additional 23 emerging PFAS in **Table S10** that had lower identification confidence (levels 3c-d, 4, and 5a-b)⁹².

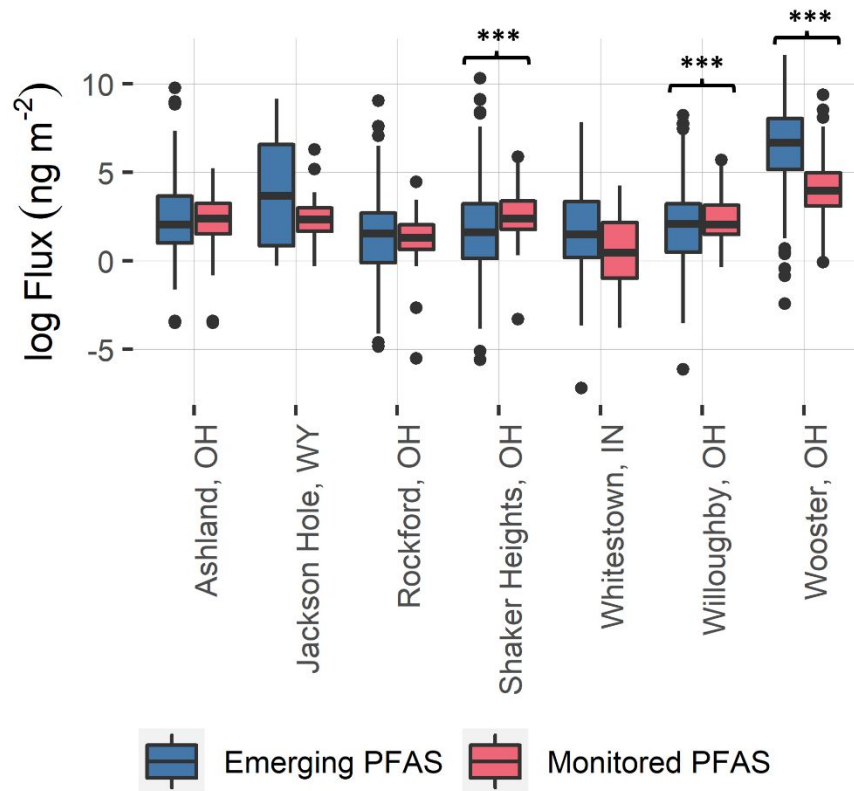


Figure 4. Boxplot comparing log flux (in ng m^{-2}) of emerging and monitored PFAS at each site. Black asterisks indicate that emerging and monitored PFAS are statistically different ($p < 0.05$) at that site.

Chain Length. According to a Kruskal-Wallis test for chain length and site location, several sites had significantly different levels (Tables S15 and S16) of ultra-short PFAS (C2-C3) in comparison to short-chain (C4-C7) and long-chain ($\geq C8$) PFAS. As shown in Figure S7, the estimated deposition fluxes of ultra-short PFAS greatly exceeded the estimated deposition fluxes of other PFAS detected in the precipitation samples collected at Ashland, Jackson Hole, and Shaker Heights. This trend matches earlier measurements of trifluoroacetic acid (TFA, C2) and PFPrA (C3) in rainwater in which the concentrations of ultrashort PFCAs greatly exceeded the concentrations of longer-chain PFCAs.^{26,31,32,38,39,114} The ultra-short chain PFAS are likely

1
2
3 present in precipitation at such high levels because these small molecules have higher vapor
4 pressures and are more water-soluble than longer-chain PFAS. Accordingly, TFA and PFPrA are
5 more likely to enter the atmosphere through volatilization and subsequently partition into
6 aqueous aerosol particles or cloud droplets. Furthermore, ultra-short PFAS are readily formed
7 from reactions of other fluorinated species, such as longer-chain PFAS or from the
8 hydrochlorofluorocarbons (HCFCs) and hydrofluorocarbons (HFCs) used as refrigerants.^{2,115}
9 TFA in particular is ubiquitous in all compartments of the environment, including rainwater.^{115–}
10
11
12
13
14
15
16
17
18
19 117

20
21 ***Functional Class.*** A Kruskal-Wallis test for functional class and location indicated that
22 each sampling site displayed significant differences in PFAS profile according to functional
23 class. Notably, the estimated deposition fluxes of FTCAs and H-PFCAs at Wooster are
24 significantly greater than the fluxes of most other functional classes (**Figure S8, Tables S17 and**
25 **S18**). In a related analysis, **Figure S9** illustrates differences in estimated deposition flux for each
26 functional class across all sampling sites. Wooster had a significantly different deposition profile
27 of FTCAs, FTUCAs, H-PFCAs, H-PFdiCAs, oPFSAs, and PFCAs when compared to all other
28 sampling sites (See **Tables S19 and S20** for data and **Table S1** for acronyms). The differences in
29 estimated deposition are particularly interesting for the sites located in close proximity. As
30 shown in **Figure S1**, Shaker Heights, Rockford, Ashland, and Willoughby are all located within
31 280 km of Wooster. The differences in functional class profiles found in precipitation at these
32 sites further support the hypothesis that elevated PFAS deposition in Wooster is a localized
33 phenomenon.
34
35
36
37
38
39
40
41
42
43
44
45
46
47
48
49
50

51 ***PFAS Correlations.*** Kendall's tau correlation was employed to examine the relationship
52 between the estimated deposition fluxes of individual PFAS at each site. **Table S21** highlights
53
54
55
56
57
58
59
60

1
2
3 particularly strong correlations ($\tau > 0.80$). PFAS with strong positive correlations may have
4 originated from the same source, though origins cannot be proved through correlations alone.
5
6
7
8 Wooster had the greatest number of correlations between compounds, which can be divided into
9
10 the two distinct groups listed in **Table S22**. First, compounds **1, 2, 3, and 12** (Group A) were all
11 strongly and positively correlated to one another. Functional classes of the Group A PFAS vary;
12 however, three of the four PFAS are short-chain, while the fourth is ultra-short. Group B consists
13 of 15 PFAS. Again, the functional classes of these compounds vary greatly, but all have a long
14 chain length. The A and B groupings, which are defined by their strong correlations and chain
15 lengths, suggest short-chain and long-chain PFAS detected in Wooster could have different
16 origins—either different emission sources or different atmospheric formation routes.
17
18
19
20
21
22
23
24
25

26 ***Principal Component Analysis.*** Principal component analysis was performed on the
27 precipitation samples to visualize similarities between sample compositions, again with the goal
28 of gaining insight into PFAS origins. The first principal component (PC1) explains 96% of the
29 variation in the data, while the second principal component (PC2) accounts for 3% of the
30 variation (**Figure S10**). The cumulative variation explained by the first two components is 99%.
31
32
33
34
35
36
37

38 **Figure S11** clearly shows the anomalous nature of the samples collected in Wooster.
39
40 While all other samples lie primarily in proximity to zero in PC1, the samples from Wooster are
41 more distributed along this axis. PC1 was strongly correlated (coefficient > 0.90) to 25 PFAS
42 (see **Table S23**). The estimated deposition fluxes of these compounds distinguished Wooster
43 from other sampling sites. In addition, the sample collected in Wooster on 6 July 2019 is vastly
44 different from all other samples and is clearly visible in **Figure S11** as an outlier along PC1. This
45 particular date was a key focus of our air mass back trajectory analysis, discussed later. Along
46 PC2, sites other than Wooster displayed more spatial variability in **Figure S11**. TFA, PFHpS
47
48
49
50
51
52
53
54
55
56
57
58
59
60

1
2
3 (16), and HFPO-DA most significantly contributed to PC2, suggesting that the deposition of
4 these compounds across sites varies widely. In summary, PCA clearly highlights yet again the
5 anomalous deposition flux of PFAS in Wooster.
6
7
8
9

10 11 **Air Mass Back Trajectories**

12
13
14 We turned to air mass back trajectories for further site-specific insights into whether
15 regional atmospheric transport affected PFAS deposition profiles. The frequency plots in
16 Appendix B of the Supporting Information show regions where the majority of air masses have
17 crossed. In general, air masses approached the collection sites from the west. At each site, we
18 compared back trajectories on days with high PFAS levels (defined as $\Sigma_{\text{PFAS}} > 50\%$ of the
19 maximum Σ_{PFAS} deposition flux) and on days with low PFAS levels (defined as $\Sigma_{\text{PFAS}} \leq 50\%$ of
20 the maximum Σ_{PFAS} deposition flux). For most Ohio sites, days with elevated PFAS levels
21 exhibited more influence from air masses passing over Michigan: More than 25% of trajectories
22 crossed Michigan on high PFAS days in Ashland, Shaker Heights, Rockford, and Willoughby.
23
24 Southwestern influences also contributed to air masses on elevated PFAS deposition days: More
25 than 25% of trajectories crossed western Illinois on high PFAS days in Rockford, and more than
26 25% of trajectories crossed Arkansas, Missouri, and Illinois on high PFAS days in Ashland and
27 Wooster. We caution that air mass back trajectories are not direct indications of PFAS origins;
28 rather, the frequency plots in Appendix B are intended to simply illustrate patterns in
29 meteorological conditions. Although it is reasonable to detect high PFAS levels in precipitation
30 from air masses that have crossed Michigan, where PFAS contamination from industrial
31 activities is well-established,¹¹⁸ such evidence is circumstantial for rainwater from the Ohio sites.
32
33 Insufficient samples were collected to identify trends in air mass trajectories at Jackson Hole,
34 WY or Whitestown, IN.
35
36
37
38
39
40
41
42
43
44
45
46
47
48
49
50
51
52
53
54
55
56
57
58
59
60

1
2
3 Curiously, PFAS levels in precipitation from Wooster were about an order of magnitude
4
5 higher in the 6 July 2019 sample than in any other sample. The estimated total PFAS deposition
6
7 flux and total concentration were $7.48 \times 10^5 \text{ ng m}^{-2}$ and $1.82 \times 10^4 \text{ ng L}^{-1}$, respectively, on July
8
9 6th in comparison to median values of $4.41 \times 10^4 \text{ ng m}^{-2}$ and $4.69 \times 10^3 \text{ ng L}^{-1}$ for the Wooster
10
11 site overall. Even though the July 6th sample from Wooster was an egregious outlier on the PCA
12
13 plot (**Figure S11**), the air mass frequency map for July 6 showed roughly the same patterns as
14
15 the maps on the other nine sampling dates in Wooster (see **Figure B7** in the Supporting
16
17 Information). We conclude that, at least at the Wooster site, local sources dominated over
18
19 background deposition of PFAS from atmospheric transport.
20
21
22
23
24
25

26 CONCLUSIONS

27
28
29 Data here show that emerging compounds may make up a majority of total PFAS load in
30
31 precipitation and potentially elsewhere in the environment if cumulative deposition from the
32
33 atmosphere is significant. However, instrumentation to conduct high-resolution mass spectral
34
35 analysis is not widely accessible for routine testing, and data analysis is time-consuming.⁶³
36
37
38

39
40
41 Further measurements of emerging PFAS can be used to generate targeted analyte lists of
42
43 representative compounds that, in conjunction with legacy monitored analytes, should more
44
45 accurately estimate total PFAS fluxes. Branched isomers also require further study. The
46
47
48
49 chromatographically distinct mixtures of PFAS observed in non-targeted analysis highlight the
50
51
52
53
54
55
56
57
58
59
60 need for a wider range of PFAS standards. Standards that include branched isomers would be

1
2
3 especially helpful to confirm the identity of mass-identical, chromatographically distinct
4
5
6
7 features, which would subsequently improve the understanding of PFAS mixtures for source
8
9
10 identification. The structural complexity of the emerging PFAS detected also suggests a need for
11
12
13 improved structural databases of manufactured fluorochemicals. In addition, understanding how
14
15
16 fluorochemicals are chemically transformed, either by an industrial process or through reactions
17
18
19 in the atmosphere, may be useful to explain the structural diversity of PFAS detected in
20
21
22 precipitation. Toxicological data should be collected to understand the risks of the emerging
23
24
25 PFAS. If the high concentration of emerging PFAS in Wooster, OH is due to incomplete
26
27
28 incineration of PFAS, then the data highlight the critical need to study and optimize thermal
29
30
31 mechanisms to mineralize PFAS and prevent emission of fluorochemicals.
32
33
34
35
36
37
38

39 **CONFLICTS OF INTEREST**

40
41 There are no conflicts to declare.
42
43
44
45

46 **ACKNOWLEDGMENTS**

47
48 This work was supported by the National Science Foundation (grant number CHE-2017788), by
49
50 the Strategic Environmental Research and Development Program (grant number ER13-1800),
51
52 and by The College of Wooster Copeland Fund. The authors would like to thank Judy
53
54
55
56
57
58
59
60

Amburgey-Peters, Betsy Bernfeld, Claire Hefner, the Pikes, the Sapps, and the Sutherlands for collecting water samples.

REFERENCES

- 1 J. Glüge, M. Scheringer, I. T. Cousins, J. C. DeWitt, G. Goldenman, D. Herzke, R. Lohmann, C. A. Ng, X. Trier and Z. Wang, An overview of the uses of per- and polyfluoroalkyl substances (PFAS), *Environ. Sci.: Processes Impacts*, 2020, **22**, 2345–2373.
- 2 C. J. Young and S. A. Mabury, in *Reviews of Environmental Contamination and Toxicology*, ed. P. De Voogt, Springer New York, New York, NY, 2010, vol. 208, pp. 1–109.
- 3 A. B. Radi, K. E. Noll and A. K. Oskouie, Per- and Polyfluoroalkyl Substances: Background Information with Focus on Modeling of Fate and Transport of Per- and Polyfluoroalkyl Substances in Air Media, *J. Environ. Eng.*, 2022, **148**, 03122001.
- 4 J. M. Armitage, U. Schenker, M. Scheringer, J. W. Martin, M. MacLeod and I. T. Cousins, Modeling the Global Fate and Transport of Perfluorooctane Sulfonate (PFOS) and Precursor Compounds in Relation to Temporal Trends in Wildlife Exposure, *Environ. Sci. Technol.*, 2009, **43**, 9274–9280.
- 5 J. J. MacInnis, I. Lehnerr, D. C. G. Muir, K. A. St. Pierre, V. L. St. Louis, C. Spencer and A. O. De Silva, Fate and Transport of Perfluoroalkyl Substances from Snowpacks into a Lake in the High Arctic of Canada, *Environ. Sci. Technol.*, 2019, **53**, 10753–10762.
- 6 C. P. Thackray, N. E. Selin and C. J. Young, A global atmospheric chemistry model for the fate and transport of PFCAs and their precursors, *Environ. Sci.: Processes Impacts*, 2020, **22**, 285–293.
- 7 B. Sha, J. H. Johansson, P. Tunved, P. Bohlin-Nizzetto, I. T. Cousins and M. E. Salter, Sea Spray Aerosol (SSA) as a Source of Perfluoroalkyl Acids (PFAAs) to the Atmosphere: Field Evidence from Long-Term Air Monitoring, *Environ. Sci. Technol.*, 2022, **56**, 228–238.
- 8 J. A. Faust, PFAS on atmospheric aerosol particles: a review, *Environ. Sci.: Processes Impacts*, 2022, 10.1039.D2EM00002D.
- 9 I. T. Cousins, J. H. Johansson, M. E. Salter, B. Sha and M. Scheringer, Outside the Safe Operating Space of a New Planetary Boundary for Per- and Polyfluoroalkyl Substances (PFAS), *Environ. Sci. Technol.*, 2022, **56**, 11172–11179.
- 10 C. J. Young, V. I. Furdui, J. Franklin, R. M. Koerner, D. C. G. Muir and S. A. Mabury, Perfluorinated Acids in Arctic Snow: New Evidence for Atmospheric Formation, *Environ. Sci. Technol.*, 2007, **41**, 3455–3461.
- 11 N. L. Stock, V. I. Furdui, D. C. G. Muir and S. A. Mabury, Perfluoroalkyl Contaminants in the Canadian Arctic: Evidence of Atmospheric Transport and Local Contamination, *Environ. Sci. Technol.*, 2007, **41**, 3529–3536.

- 12 C. M. Butt, U. Berger, R. Bossi and G. T. Tomy, Levels and trends of poly- and perfluorinated compounds in the arctic environment, *Sci. Total Environ.*, 2010, **408**, 2936–2965.
- 13 L. Ahrens, M. Shoeib, S. Del Vento, G. Codling and C. Halsall, Polyfluoroalkyl compounds in the Canadian Arctic atmosphere, *Environ. Chem.*, 2011, **8**, 399–406.
- 14 P. Casal, Y. Zhang, J. W. Martin, M. Pizarro, B. Jiménez and J. Dachs, Role of Snow Deposition of Perfluoroalkylated Substances at Coastal Livingston Island (Maritime Antarctica), *Environ. Sci. Technol.*, 2017, **51**, 8460–8470.
- 15 G. Casas, A. Martínez-Varela, M. Vila-Costa, B. Jiménez and J. Dachs, Rain Amplification of Persistent Organic Pollutants, *Environ. Sci. Technol.*, 2021, **55**, 12961–12972.
- 16 S. Taniyasu, N. Yamashita, H.-B. Moon, K. Y. Kwok, P. K. S. Lam, Y. Horii, G. Petrick and K. Kannan, Does wet precipitation represent local and regional atmospheric transportation by perfluorinated alkyl substances?, *Environ. Int.*, 2013, **55**, 25–32.
- 17 E. M. Sunderland, X. C. Hu, C. Dassuncao, A. K. Tokranov, C. C. Wagner and J. G. Allen, A review of the pathways of human exposure to poly- and perfluoroalkyl substances (PFASs) and present understanding of health effects, *J. Exposure Sci. Environ. Epidemiol.*, 2019, **29**, 131–147.
- 18 S. E. Fenton, A. Ducatman, A. Boobis, J. C. DeWitt, C. Lau, C. Ng, J. S. Smith and S. M. Roberts, Per- and Polyfluoroalkyl Substance Toxicity and Human Health Review: Current State of Knowledge and Strategies for Informing Future Research, *Environ. Toxicol. Chem.*, 2021, **40**, 606–630.
- 19 A. O. De Silva, J. M. Armitage, T. A. Bruton, C. Dassuncao, W. Heiger-Bernays, X. C. Hu, A. Kärman, B. Kelly, C. Ng, A. Robuck, M. Sun, T. F. Webster and E. M. Sunderland, PFAS Exposure Pathways for Humans and Wildlife: A Synthesis of Current Knowledge and Key Gaps in Understanding, *Environ. Toxicol. Chem.*, 2021, **40**, 631–657.
- 20 G. T. Ankley, P. Cureton, R. A. Hoke, M. Houde, A. Kumar, J. Kurias, R. Lanno, C. McCarthy, J. Newsted, C. J. Salice, B. E. Sample, M. S. Sepúlveda, J. Steevens and S. Valsecchi, Assessing the Ecological Risks of Per- and Polyfluoroalkyl Substances: Current State-of-the Science and a Proposed Path Forward, *Environ. Toxicol. Chem.*, 2021, **40**, 564–605.
- 21 M. G. Evich, M. J. B. Davis, J. P. McCord, B. Acrey, J. A. Awkerman, D. R. U. Knappe, A. B. Lindstrom, T. F. Speth, C. Tebes-Stevens, M. J. Strynar, Z. Wang, E. J. Weber, W. M. Henderson and J. W. Washington, Per- and polyfluoroalkyl substances in the environment, *Science*, 2022, **375**, eabg9065.
- 22 C. A. Barton, M. A. Kaiser and M. H. Russell, Partitioning and removal of perfluorooctanoate during rain events: The importance of physical-chemical properties, *J. Environ. Monit.*, 2007, **9**, 839–846.
- 23 W. Liu, Y. Jin, X. Quan, K. Sasaki, N. Saito, S. F. Nakayama, I. Sato and S. Tsuda, Perfluorosulfonates and perfluorocarboxylates in snow and rain in Dalian, China, *Environ. Int.*, 2009, **35**, 737–742.

- 1
2
3 24 J. H. Johansson, Y. Shi, M. Salter and I. T. Cousins, Spatial variation in the atmospheric
4 deposition of perfluoroalkyl acids: source elucidation through analysis of isomer patterns,
5 *Environ. Sci.: Processes Impacts*, 2018, **20**, 997–1006.
6
- 7 25 M. Chen, C. Wang, K. Gao, X. Wang, J. Fu, P. Gong and Y. Wang, Perfluoroalkyl
8 substances in precipitation from the Tibetan Plateau during monsoon season: Concentrations,
9 source regions and mass fluxes, *Chemosphere*, 2021, **282**, 131105.
10
- 11 26 B. F. Scott, C. A. Moody, C. Spencer, J. M. Small, D. C. G. Muir and S. A. Mabury,
12 Analysis for Perfluorocarboxylic Acids/Anions in Surface Waters and Precipitation Using
13 GC–MS and Analysis of PFOA from Large-Volume Samples, *Environ. Sci. Technol.*, 2006,
14 **40**, 6405–6410.
15
- 16 27 A. O. De Silva, D. C. G. Muir and S. A. Mabury, Distribution of Perfluorocarboxylate
17 Isomers in Select Samples from the North American Environment, *Environ. Toxicol. Chem.*,
18 2009, **28**, 1801–1814.
19
- 20 28 S. B. Gewurtz, L. E. Bradley, S. Backus, A. Dove, D. McGoldrick, H. Hung and H.
21 Dryfhout-Clark, Perfluoroalkyl Acids in Great Lakes Precipitation and Surface Water (2006–
22 2018) Indicate Response to Phase-outs, Regulatory Action, and Variability in Fate and
23 Transport Processes, *Environ. Sci. Technol.*, 2019, **53**, 8543–8552.
24
- 25 29 C. E. Müller, N. Spiess, A. C. Gerecke, M. Scheringer and K. Hungerbühler, Quantifying
26 Diffuse and Point Inputs of Perfluoroalkyl Acids in a Nonindustrial River Catchment,
27 *Environ. Sci. Technol.*, 2011, **45**, 9901–9909.
28
- 29 30 G. Sammut, E. Sinagra, R. Helmus and P. de Voogt, Perfluoroalkyl substances in the
30 Maltese environment – (I) surface water and rain water, *Sci. Total Environ.*, 2017, **589**, 182–
31 190.
32
- 33 31 S. Taniyasu, K. Kannan, L. W. Y. Yeung, K. Y. Kwok, P. K. S. Lam and N. Yamashita,
34 Analysis of trifluoroacetic acid and other short-chain perfluorinated acids (C2–C4) in
35 precipitation by liquid chromatography–tandem mass spectrometry: Comparison to patterns
36 of long-chain perfluorinated acids (C5–C18), *Anal. Chim. Acta*, 2008, **619**, 221–230.
37
- 38 32 K. A. Pike, P. L. Edmiston, J. J. Morrison and J. A. Faust, Correlation Analysis of
39 Perfluoroalkyl Substances in Regional U.S. Precipitation Events, *Water Res.*, 2021, **190**,
40 116685.
41
- 42 33 M. S. Shimizu, R. Mott, A. Potter, J. Zhou, K. Baumann, J. D. Surratt, B. Turpin, G. B.
43 Avery, J. Harfmann, R. J. Kieber, R. N. Mead, S. A. Skrabal and J. D. Willey, Atmospheric
44 Deposition and Annual Flux of Legacy Perfluoroalkyl Substances and Replacement
45 Perfluoroalkyl Ether Carboxylic Acids in Wilmington, NC, USA, *Environ. Sci. Technol.*
46 *Lett.*, 2021, **8**, 366–372.
47
- 48 34 K. Y. Kwok, S. Taniyasu, L. W. Y. Yeung, M. B. Murphy, P. K. S. Lam, Y. Horii, K.
49 Kannan, G. Petrick, R. K. Sinha and N. Yamashita, Flux of Perfluorinated Chemicals
50 through Wet Deposition in Japan, the United States, And Several Other Countries, *Environ.*
51 *Sci. Technol.*, 2010, **44**, 7043–7049.
52
- 53 35 L. Zhao, M. Zhou, T. Zhang and H. Sun, Polyfluorinated and Perfluorinated Chemicals in
54 Precipitation and Runoff from Cities Across Eastern and Central China, *Arch. Environ.*
55 *Contam. Toxicol.*, 2013, **64**, 198–207.
56
57
58
59
60

- 1
2
3 36 A. Dreyer, V. Matthias, I. Weinberg and R. Ebinghaus, Wet deposition of poly- and
4 perfluorinated compounds in Northern Germany, *Environ. Pollut.*, 2010, **158**, 1221–1227.
5
6 37 M. Loewen, T. Halldorson, F. Wang and G. Tomy, Fluorotelomer Carboxylic Acids and
7 PFOS in Rainwater from an Urban Center in Canada, *Environ. Sci. Technol.*, 2005, **39**,
8 2944–2951.
9
10 38 B. F. Scott, C. Spencer, S. A. Mabury and D. C. G. Muir, Poly and Perfluorinated
11 Carboxylates in North American Precipitation, *Environ. Sci. Technol.*, 2006, **40**, 7167–7174.
12
13 39 H. Chen, L. Zhang, M. Li, Y. Yao, Z. Zhao, G. Munoz and H. Sun, Per- and polyfluoroalkyl
14 substances (PFASs) in precipitation from mainland China: Contributions of unknown
15 precursors and short-chain (C2 C3) perfluoroalkyl carboxylic acids, *Water Res.*, 2019, **153**,
16 169–177.
17
18 40 J. P. Koelmel, P. Stelben, C. A. McDonough, D. A. Dukes, J. J. Aristizabal-Henao, S. L.
19 Nason, Y. Li, S. Sternberg, E. Lin, M. Beckmann, A. J. Williams, J. Draper, J. P. Finch, J. K.
20 Munk, C. Deigl, E. E. Rennie, J. A. Bowden and K. J. Godri Pollitt, FluoroMatch 2.0—
21 making automated and comprehensive non-targeted PFAS annotation a reality, *Anal.*
22 *Bioanal. Chem.*, 2022, **414**, 1201–1215.
23
24 41 Z. Wang, J. C. DeWitt, C. P. Higgins and I. T. Cousins, A Never-Ending Story of Per- and
25 Polyfluoroalkyl Substances (PFASs)?, *Environ. Sci. Technol.*, 2017, **51**, 2508–2518.
26
27 42 Z. Wang, A. M. Buser, I. T. Cousins, S. Demattio, W. Drost, O. Johansson, K. Ohno, G.
28 Patlewicz, A. M. Richard, G. W. Walker, G. S. White and E. Leinala, A New OECD
29 Definition for Per- and Polyfluoroalkyl Substances, *Environ. Sci. Technol.*, 2021, **55**, 15575–
30 15578.
31
32 43 M. Sun, E. Arevalo, M. Strynar, A. Lindstrom, M. Richardson, B. Kearns, A. Pickett, C.
33 Smith and D. R. U. Knappe, Legacy and Emerging Perfluoroalkyl Substances Are Important
34 Drinking Water Contaminants in the Cape Fear River Watershed of North Carolina, *Environ.*
35 *Sci. Technol. Lett.*, 2016, **3**, 415–419.
36
37 44 T. Ruan and G. Jiang, Analytical methodology for identification of novel per- and
38 polyfluoroalkyl substances in the environment, *TrAC Trends Anal. Chem.*, 2017, **95**, 122–
39 131.
40
41 45 R. A. Brase, E. J. Mullin and D. C. Spink, Legacy and Emerging Per- and Polyfluoroalkyl
42 Substances: Analytical Techniques, Environmental Fate, and Health Effects, *Int. J. Mol. Sci.*,
43 2021, **22**, 995.
44
45 46 M. Liu, G. Munoz, S. Vo Duy, S. Sauvé and J. Liu, Per- and Polyfluoroalkyl Substances in
46 Contaminated Soil and Groundwater at Airports: A Canadian Case Study, *Environ. Sci.*
47 *Technol.*, 2022, **56**, 885–895.
48
49 47 Y. Liu, L. A. D'Agostino, G. Qu, G. Jiang and J. W. Martin, High-resolution mass
50 spectrometry (HRMS) methods for nontarget discovery and characterization of poly- and
51 per-fluoroalkyl substances (PFASs) in environmental and human samples, *TrAC Trends*
52 *Anal. Chem.*, 2019, **121**, 115420.
53
54 48 J. L. Guelfo, S. Korzeniowski, M. A. Mills, J. Anderson, R. H. Anderson, J. A. Arblaster, J.
55 M. Conder, I. T. Cousins, K. Dasu, B. J. Henry, L. S. Lee, J. Liu, E. R. McKenzie and J.
56
57
58
59
60

- 1
2
3 Willey, Environmental Sources, Chemistry, Fate, and Transport of Per- and Polyfluoroalkyl
4 Substances: State of the Science, Key Knowledge Gaps, and Recommendations Presented at
5 the August 2019 SETAC Focus Topic Meeting, *Environ. Toxicol. Chem.*, 2021, **40**, 3234–
6 3260.
7
- 8 49 S. Jia, M. Marques Dos Santos, C. Li and S. A. Snyder, Recent advances in mass
9 spectrometry analytical techniques for per- and polyfluoroalkyl substances (PFAS), *Anal.*
10 *Bioanal. Chem.*, 2022, **414**, 2795–2807.
11
- 12 50 J. Aceña, S. Stampachiachiere, S. Pérez and D. Barceló, Advances in liquid
13 chromatography–high-resolution mass spectrometry for quantitative and qualitative
14 environmental analysis, *Anal. Bioanal. Chem.*, 2015, **407**, 6289–6299.
15
- 16 51 B. González-Gaya, N. Lopez-Herguedas, D. Bilbao, L. Mijangos, A. M. Iker, N. Etxebarria,
17 M. Irazola, A. Prieto, M. Olivares and O. Zuloaga, Suspect and non-target screening: the last
18 frontier in environmental analysis, *Anal. Methods*, 2021, **13**, 1876–1904.
19
- 20 52 S. Newton, R. McMahan, J. A. Stoeckel, M. Chislock, A. Lindstrom and M. Strynar, Novel
21 Polyfluorinated Compounds Identified Using High Resolution Mass Spectrometry
22 Downstream of Manufacturing Facilities near Decatur, Alabama, *Environ. Sci. Technol.*,
23 2017, **51**, 1544–1552.
24
- 25 53 J. P. McCord, M. J. Strynar, J. W. Washington, E. L. Bergman and S. M. Goodrow,
26 Emerging Chlorinated Polyfluorinated Polyether Compounds Impacting the Waters of
27 Southwestern New Jersey Identified by Use of Nontargeted Analysis, *Environ. Sci. Technol.*
28 *Lett.*, 2020, **7**, 903–908.
29
- 30 54 S. Yukioka, S. Tanaka, Y. Suzuki, S. Echigo, A. Kärman and S. Fujii, A profile analysis
31 with suspect screening of per- and polyfluoroalkyl substances (PFASs) in firefighting foam
32 impacted waters in Okinawa, Japan, *Water Res.*, 2020, **184**, 116207.
33
- 34 55 R. Gonzalez de Vega, A. Cameron, D. Clases, T. M. Dodgen, P. A. Doble and D. P. Bishop,
35 Simultaneous targeted and non-targeted analysis of per- and polyfluoroalkyl substances in
36 environmental samples by liquid chromatography-ion mobility-quadrupole time of flight-
37 mass spectrometry and mass defect analysis, *J. Chromatogr. A*, 2021, **1653**, 462423.
38
- 39 56 J. Yao, N. Sheng, Y. Guo, L. W. Y. Yeung, J. Dai and Y. Pan, Nontargeted Identification
40 and Temporal Trends of Per- and Polyfluoroalkyl Substances in a Fluorochemical Industrial
41 Zone and Adjacent Taihu Lake, *Environ. Sci. Technol.*, 2022, **56**, 7986–7996.
42
- 43 57 Y. Wang, N. Yu, X. Zhu, H. Guo, J. Jiang, X. Wang, W. Shi, J. Wu, H. Yu and S. Wei,
44 Suspect and Nontarget Screening of Per- and Polyfluoroalkyl Substances in Wastewater
45 from a Fluorochemical Manufacturing Park, *Environ. Sci. Technol.*, 2018, **52**, 11007–11016.
46
- 47 58 P. Jacob, K. A. Barzen-Hanson and D. E. Helbling, Target and Nontarget Analysis of Per-
48 and Polyfluoroalkyl Substances in Wastewater from Electronics Fabrication Facilities,
49 *Environ. Sci. Technol.*, 2021, **55**, 2346–2356.
50
- 51 59 X. Wang, N. Yu, Y. Qian, W. Shi, X. Zhang, J. Geng, H. Yu and S. Wei, Non-target and
52 suspect screening of per- and polyfluoroalkyl substances in Chinese municipal wastewater
53 treatment plants, *Water Res.*, 2020, **183**, 115989.
54
55
56
57
58
59
60

- 1
2
3
4
5
6
7
8
9
10
11
12
13
14
15
16
17
18
19
20
21
22
23
24
25
26
27
28
29
30
31
32
33
34
35
36
37
38
39
40
41
42
43
44
45
46
47
48
49
50
51
52
53
54
55
56
57
58
59
60
- 60 Y. Jeong, K. M. Da Silva, E. Iturraspe, Y. Fuiji, T. Boogaerts, A. L. N. van Nuijs, J. Koelmel and A. Covaci, Occurrence and contamination profile of legacy and emerging per- and polyfluoroalkyl substances (PFAS) in Belgian wastewater using target, suspect and non-target screening approaches, *J. Hazard Mater.*, 2022, **437**, 129378.
- 61 N. Yu, H. Guo, J. Yang, L. Jin, X. Wang, W. Shi, X. Zhang, H. Yu and S. Wei, Non-Target and Suspect Screening of Per- and Polyfluoroalkyl Substances in Airborne Particulate Matter in China, *Environ. Sci. Technol.*, 2018, **52**, 8205–8214.
- 62 N. Yu, H. Wen, X. Wang, E. Yamazaki, S. Taniyasu, N. Yamashita, H. Yu and S. Wei, Nontarget Discovery of Per- and Polyfluoroalkyl Substances in Atmospheric Particulate Matter and Gaseous Phase Using Cryogenic Air Sampler, *Environ. Sci. Technol.*, 2020, **54**, 3103–3113.
- 63 M. J. Benotti, L. A. Fernandez, G. F. Peaslee, G. S. Douglas, A. D. Uhler and S. Emsbo-Mattingly, A forensic approach for distinguishing PFAS materials, *Environ. Forensics*, 2020, **21**, 319–333.
- 64 J. A. Charbonnet, A. E. Rodowa, N. T. Joseph, J. L. Guelfo, J. A. Field, G. D. Jones, C. P. Higgins, D. E. Helbling and E. F. Houtz, Environmental Source Tracking of Per- and Polyfluoroalkyl Substances within a Forensic Context: Current and Future Techniques, *Environ. Sci. Technol.*, 2021, **55**, 7237–7245.
- 65 J. P. Benskin, A. O. De Silva and J. W. Martin, in *Reviews of Environmental Contamination and Toxicology Volume 208*, ed. P. De Voogt, Springer New York, New York, NY, 2010, vol. 208, pp. 111–160.
- 66 K. Schulz, M. R. Silva and R. Klaper, Distribution and effects of branched versus linear isomers of PFOA, PFOS, and PFHxS: A review of recent literature, *Sci. Total Environ.*, 2020, **733**, 139186.
- 67 S. Rayne, K. Forest and K. J. Friesen, Estimated congener specific gas-phase atmospheric behavior and fractionation of perfluoroalkyl compounds: Rates of reaction with atmospheric oxidants, air-water partitioning, and wet/dry deposition lifetimes, *J. Environ. Sci. Health, Part A*, 2009, **44**, 936–954.
- 68 D. D. Perrin, B. Dempsey and E. P. Serjeant, *pK_a Prediction for Organic Acids and Bases*, Springer Netherlands, Dordrecht, 1981.
- 69 D. C. Burns, D. A. Ellis, H. Li, C. J. McMurdo and E. Webster, Experimental pK_a Determination for Perfluorooctanoic Acid (PFOA) and the Potential Impact of pK_a Concentration Dependence on Laboratory-Measured Partitioning Phenomena and Environmental Modeling, *Environ. Sci. Technol.*, 2008, **42**, 9283–9288.
- 70 Z. Wang, M. MacLeod, I. T. Cousins, M. Scheringer and K. Hungerbühler, Using COSMOtherm to predict physicochemical properties of poly- and perfluorinated alkyl substances (PFASs), *Environ. Chem.*, 2011, **8**, 389–398.
- 71 A. Kärman, K. Elgh-Dalgren, C. Lafossas and T. Møskeland, Environmental levels and distribution of structural isomers of perfluoroalkyl acids after aqueous fire-fighting foam (AFFF) contamination, *Environ. Chem.*, 2011, **8**, 372–380.

- 1
2
3 72 X. Chen, L. Zhu, X. Pan, S. Fang, Y. Zhang and L. Yang, Isomeric specific partitioning
4 behaviors of perfluoroalkyl substances in water dissolved phase, suspended particulate
5 matters and sediments in Liao River Basin and Taihu Lake, China, *Water Res.*, 2015, **80**,
6 235–244.
7
- 8 73 Y. Gao, Y. Liang, K. Gao, Y. Wang, C. Wang, J. Fu, Y. Wang, G. Jiang and Y. Jiang,
9 Levels, spatial distribution and isomer profiles of perfluoroalkyl acids in soil, groundwater
10 and tap water around a manufactory in China, *Chemosphere*, 2019, **227**, 305–314.
11
- 12 74 S. Fang, B. Sha, H. Yin, Y. Bian, B. Yuan and I. T. Cousins, Environment occurrence of
13 perfluoroalkyl acids and associated human health risks near a major fluorochemical
14 manufacturing park in southwest of China, *J. Hazard Mater.*, 2020, **396**, 122617.
15
- 16 75 H. A. Langberg, H. P. H. Arp, G. D. Breedveld, G. A. Slinde, Å. Høiseter, H. M. Grønning,
17 M. Jartun, T. Rundberget, B. M. Jenssen and S. E. Hale, Paper product production identified
18 as the main source of per- and polyfluoroalkyl substances (PFAS) in a Norwegian lake:
19 Source and historic emission tracking, *Environ. Pollut.*, 2021, **273**, 116259.
20
- 21 76 J. P. Benskin, V. Phillips, V. L. St. Louis and J. W. Martin, Source Elucidation of
22 Perfluorinated Carboxylic Acids in Remote Alpine Lake Sediment Cores, *Environ. Sci.*
23 *Technol.*, 2011, **45**, 7188–7194.
24
- 25 77 S. Fang, C. Li, L. Zhu, H. Yin, Y. Yang, Z. Ye and I. T. Cousins, Spatiotemporal distribution
26 and isomer profiles of perfluoroalkyl acids in airborne particulate matter in Chengdu City,
27 China, *Sci. Total Environ.*, 2019, **689**, 1235–1243.
28
- 29 78 J. Wu, H. Jin, L. Li, Z. Zhai, J. W. Martin, J. Hu, L. Peng and P. Wu, Atmospheric
30 perfluoroalkyl acid occurrence and isomer profiles in Beijing, China, *Environ. Pollut.*, 2019,
31 **255**, 113129.
32
- 33 79 B. Place, 2021, Suspect List of Possible Per-and Polyfluoroalkyl Substances (PFAS) version
34 1.5.0, National Institute of Standards and Technology, DOI: 10.18434/MDS2-2387.
35
- 36 80 B. Bugsel and C. Zwiener, LC-MS screening of poly- and perfluoroalkyl substances in
37 contaminated soil by Kendrick mass analysis, *Anal. Bioanal. Chem.*, 2020, **412**, 4797–4805.
38
- 39 81 Y. Liu, A. D. S. Pereira and J. W. Martin, Discovery of C₅–C₁₇ Poly- and Perfluoroalkyl
40 Substances in Water by In-Line SPE-HPLC-Orbitrap with In-Source Fragmentation
41 Flagging, *Anal. Chem.*, 2015, **87**, 4260–4268.
42
- 43 82 R. R. Draxler and G. D. Hess, An overview of the HYSPLIT_4 modeling system of
44 trajectories, dispersion, and deposition, *Aust. Meteor. Mag.*, 1998, **47**, 295–308.
45
- 46 83 A. F. Stein, R. R. Draxler, G. D. Rolph, B. J. B. Stunder, M. D. Cohen and F. Ngan,
47 NOAA's HYSPLIT Atmospheric Transport and Dispersion Modeling System, *Bull. Am.*
48 *Meteorol. Soc.*, 2015, **96**, 2059–2077.
49
- 50 84 H. Tsugawa, T. Cajka, T. Kind, Y. Ma, B. Higgins, K. Ikeda, M. Kanazawa, J.
51 VanderGheynst, O. Fiehn and M. Arita, MS-DIAL: data-independent MS/MS deconvolution
52 for comprehensive metabolome analysis, *Nat. Methods*, 2015, **12**, 523–526.
53
- 54 85 E. N. Pieke, K. Granby, X. Trier and J. Smedsgaard, A framework to estimate concentrations
55 of potentially unknown substances by semi-quantification in liquid chromatography
56 electrospray ionization mass spectrometry, *Anal. Chim. Acta*, 2017, **975**, 30–41.
57
58
59
60

- 1
2
3 86 National Weather Service Forecast Office: Cleveland, OH, NOWData - NOAA Online
4 Weather Data, <https://w2.weather.gov/climate/xmacis.php?wfo=cle>, (accessed 13 July 2020).
5
- 6 87 BP4NTA, NTA Study Reporting Tool (PDF), *figshare*, 2022,
7 10.6084/M9.FIGSHARE.19763482.
8
- 9 88 K. T. Peter, A. L. Phillips, A. M. Knolhoff, P. R. Gardinali, C. A. Manzano, K. E. Miller, M.
10 Pristner, L. Sabourin, M. W. Sumarah, B. Warth and J. R. Sobus, Nontargeted Analysis
11 Study Reporting Tool: A Framework to Improve Research Transparency and
12 Reproducibility, *Anal. Chem.*, 2021, **93**, 13870–13879.
13
- 14 89 R Core Team, R: A Language and Environment for Statistical Computing, [https://www.R-](https://www.R-project.org/)
15 [project.org/](https://www.R-project.org/).
16
- 17 90 E. Kalnay, M. Kanamitsu, R. Kistler, W. Collins, D. Deaven, L. Gandin, M. Iredell, S. Saha,
18 G. White, J. Woollen, Y. Zhu, A. Leetmaa, R. Reynolds, M. Chelliah, W. Ebisuzaki, W.
19 Higgins, J. Janowiak, K. C. Mo, C. Ropelewski, J. Wang, R. Jenne and D. Joseph, The
20 NCEP/NCAR 40-Year Reanalysis Project, *Bull. Amer. Meteor. Soc.*, 1996, **77**, 437–471.
21
- 22 91 J. P. Koelmel, M. K. Paige, J. J. Aristizabal-Henao, N. M. Robey, S. L. Nason, P. J. Stelben,
23 Y. Li, N. M. Kroeger, M. P. Napolitano, T. Savvaides, V. Vasiliou, P. Rostkowski, T. J.
24 Garrett, E. Lin, C. Deigl, K. Jobst, T. G. Townsend, K. J. Godri Pollitt and J. A. Bowden,
25 Toward Comprehensive Per- and Polyfluoroalkyl Substances Annotation Using FluoroMatch
26 Software and Intelligent High-Resolution Tandem Mass Spectrometry Acquisition, *Anal.*
27 *Chem.*, 2020, **92**, 11186–11194.
28
- 29 92 J. A. Charbonnet, C. A. McDonough, F. Xiao, T. Schwichtenberg, D. Cao, S. Kaserzon, K.
30 V. Thomas, P. Dewapriya, B. J. Place, E. L. Schymanski, J. A. Field, D. E. Helbling and C.
31 P. Higgins, Communicating Confidence of Per- and Polyfluoroalkyl Substance Identification
32 via High-Resolution Mass Spectrometry, *Environ. Sci. Technol. Lett.*, 2022, **9**, 473–481.
33
- 34 93 H.-J. Lehmler, Synthesis of environmentally relevant fluorinated surfactants—a review,
35 *Chemosphere*, 2005, **58**, 1471–1496.
36
- 37 94 K. A. Barzen-Hanson, S. C. Roberts, S. Choyke, K. Oetjen, A. McAlees, N. Riddell, R.
38 McCrindle, P. L. Ferguson, C. P. Higgins and J. A. Field, Discovery of 40 Classes of Per-
39 and Polyfluoroalkyl Substances in Historical Aqueous Film-Forming Foams (AFFFs) and
40 AFFF-Impacted Groundwater, *Environ. Sci. Technol.*, 2017, **51**, 2047–2057.
41
- 42 95 R. A. García, A. C. Chiaia-Hernández, P. A. Lara-Martin, M. Loos, J. Hollender, K. Oetjen,
43 C. P. Higgins and J. A. Field, Suspect Screening of Hydrocarbon Surfactants in AFFFs and
44 AFFF-Contaminated Groundwater by High-Resolution Mass Spectrometry, *Environ. Sci.*
45 *Technol.*, 2019, **53**, 8068–8077.
46
- 47 96 A. Koch, S. Yukioka, S. Tanaka, L. W. Y. Yeung, A. Kärman and T. Wang,
48 Characterization of an AFFF impacted freshwater environment using total fluorine,
49 extractable organofluorine and suspect per- and polyfluoroalkyl substance screening
50 analysis, *Chemosphere*, 2021, **276**, 130179.
51
- 52 97 K.-U. Goss, The pK_a Values of PFOA and Other Highly Fluorinated Carboxylic Acids,
53 *Environ. Sci. Technol.*, 2008, **42**, 456–458.
54
55
56
57
58
59
60

- 1
2
3 98 K. Prevedouros, I. T. Cousins, R. C. Buck and S. H. Korzeniowski, Sources, Fate and
4 Transport of Perfluorocarboxylates, *Environ. Sci. Technol.*, 2006, **40**, 32–44.
5
6 99 D. A. Ellis, J. W. Martin, A. O. De Silva, S. A. Mabury, M. D. Hurley, M. P. Sulbaek
7 Andersen and T. J. Wallington, Degradation of Fluorotelomer Alcohols: A Likely
8 Atmospheric Source of Perfluorinated Carboxylic Acids, *Environ. Sci. Technol.*, 2004, **38**,
9 3316–3321.
10
11 100 M. M. Schultz, D. F. Barofsky and J. A. Field, Fluorinated Alkyl Surfactants, *Environ. Eng.*
12 *Sci.*, 2003, **20**, 487–501.
13
14 101 J. P. Benskin, M. Bataineh and J. W. Martin, Simultaneous Characterization of
15 Perfluoroalkyl Carboxylate, Sulfonate, and Sulfonamide Isomers by Liquid
16 Chromatography–Tandem Mass Spectrometry, *Anal. Chem.*, 2007, **79**, 6455–6464.
17
18 102 A. Pellizzaro, A. Zaggia, M. Fant, L. Conte and L. Falletti, Identification and quantification
19 of linear and branched isomers of perfluorooctanoic and perfluorooctane sulfonic acids in
20 contaminated groundwater in the veneto region, *J. Chromatogr. A*, 2018, **1533**, 143–154.
21
22 103 T. L. Coggan, T. Anumol, J. Pyke, J. Shimeta and B. O. Clarke, A single analytical method
23 for the determination of 53 legacy and emerging per- and polyfluoroalkyl substances (PFAS)
24 in aqueous matrices, *Anal. Bioanal. Chem.*, 2019, **411**, 3507–3520.
25
26 104 J. H. Johansson, H. Yan, U. Berger and I. T. Cousins, Water-to-air transfer of branched and
27 linear PFOA: Influence of pH, concentration and water type, *Emerging Contam.*, 2017, **3**,
28 46–53.
29
30 105 Y. Wen, Á. Rentería-Gómez, G. S. Day, M. F. Smith, T.-H. Yan, R. O. K. Ozdemir, O.
31 Gutierrez, V. K. Sharma, X. Ma and H.-C. Zhou, Integrated Photocatalytic Reduction and
32 Oxidation of Perfluorooctanoic Acid by Metal–Organic Frameworks: Key Insights into the
33 Degradation Mechanisms, *J. Am. Chem. Soc.*, 2022, **144**, 11840–11850.
34
35 106 L. J. Winchell, J. J. Ross, M. J. M. Wells, X. Fonoll, J. W. Norton and K. Y. Bell, Per- and
36 polyfluoroalkyl substances thermal destruction at water resource recovery facilities: A state
37 of the science review, *Water Environ. Res.*, 2021, **93**, 826–843.
38
39 107 J. Horst, J. McDonough, I. Ross and E. Houtz, Understanding and Managing the Potential
40 By-Products of PFAS Destruction, *Groundwater Monit. Rem.*, 2020, **40**, 17–27.
41
42 108 G. K. Longendyke, S. Katel and Y. Wang, PFAS fate and destruction mechanisms during
43 thermal treatment: a comprehensive review, *Environ. Sci.: Processes Impacts*, 2022, **24**,
44 196–208.
45
46 109 M. Altarawneh, M. H. Almatarneh and B. Z. Dlugogorski, Thermal decomposition of
47 perfluorinated carboxylic acids: Kinetic model and theoretical requirements for PFAS
48 incineration, *Chemosphere*, 2022, **286**, 131685.
49
50 110 F. Xiao, P. C. Sasi, B. Yao, A. Kubátová, S. A. Golovko, M. Y. Golovko and D. Soli,
51 Thermal Stability and Decomposition of Perfluoroalkyl Substances on Spent Granular
52 Activated Carbon, *Environ. Sci. Technol. Lett.*, 2020, **7**, 343–350.
53
54 111 U.S. Environmental Protection Agency, *Method 533: Determination of Per- and*
55 *Polyfluoroalkyl Substances in Drinking Water by Isotope Dilution Anion Exchange Solid*
56 *Phase Extraction and Liquid Chromatography/Tandem Mass Spectrometry*, 2019.
57
58
59
60

- 1
2
3 112 U.S. Environmental Protection Agency, *Method 537.1: Determination of Selected Per- and*
4 *Polyfluorinated Alkyl Substances in Drinking Water by Solid Phase Extraction and Liquid*
5 *Chromatography/Tandem Mass Spectrometry (LC/MS/MS)*, 2018.
6
7 113 Environmental Protection Agency, Lifetime Drinking Water Health Advisories for Four
8 Perfluoroalkyl Substances, *Fed. Regist.*, 2022, **87**, 36848–36849.
9
10 114 M. Berg, S. R. Müller, J. Mühlemann, A. Wiedmer and R. P. Schwarzenbach,
11 Concentrations and Mass Fluxes of Chloroacetic Acids and Trifluoroacetic Acid in Rain and
12 Natural Waters in Switzerland, *Environ. Sci. Technol.*, 2000, **34**, 2675–2683.
13
14 115 S. Joudan, A. O. De Silva and C. J. Young, Insufficient evidence for the existence of natural
15 trifluoroacetic acid, *Environ. Sci.: Processes Impacts*, 2021, **23**, 1641–1649.
16
17 116 M. Scheurer, K. Nödler, F. Freeling, J. Janda, O. Happel, M. Riegel, U. Müller, F. R. Storck,
18 M. Fleig, F. T. Lange, A. Brunsch and H.-J. Brauch, Small, mobile, persistent:
19 Trifluoroacetate in the water cycle – Overlooked sources, pathways, and consequences for
20 drinking water supply, *Water Res.*, 2017, **126**, 460–471.
21
22 117 M. Ateia, A. Maroli, N. Tharayil and T. Karanfil, The overlooked short- and ultrashort-chain
23 poly- and perfluorinated substances: A review, *Chemosphere*, 2019, **220**, 866–882.
24
25 118 R. W. Helmer, D. M. Reeves and D. P. Cassidy, Per- and Polyfluorinated Alkyl Substances
26 (PFAS) cycling within Michigan: Contaminated sites, landfills and wastewater treatment
27 plants, *Water Res.*, 2022, **210**, 117983.
28
29
30
31
32
33
34
35
36
37
38
39
40
41
42
43
44
45
46
47
48
49
50
51
52
53
54
55
56
57
58
59
60